ABSTRACT

RETRANSMISSION STRATEGIES FOR MOVING NETWORKS OVER RICEAN FADING CHANNELS

by
Alex Ruiz Lee

The problem of designing retransmission protocols based on Hybrid Automatic Repeat reQuest (HARQ) for moving networks over Ricean fading channels has been considered. The scenario of interest consists of one receiver traveling at a given speed while connected to a wireless network based on OFDM (e.g., WiMax) through several base stations located along the path. Five different retransmission protocols that combine HARQ with handover between adjacent base stations are considered. Their performance in terms of number of retransmissions per packet via numerical simulations, considering both frequency selective and nonselective channels are presented. The results obtained show the relevant advantage that can be achieved by the joint design of HARQ and handover, and by exploiting space-time transmit diversity and beamforming via softhandover.

RETRANSMISSION STRATEGIES FOR MOVING NETWORKS OVER RICEAN FADING CHANNELS

by
Alex Ruiz Lee

Blank Page

APPROVAL PAGE

RETRANSMISSION STRATEGIES FOR MOVING NETWORKS OVER RICEAN FADING CHANNELS

Alex Ruiz Lee

Dr. Yeheskel Bar-Ness, Thesis Advisor   Date
Distinguished Professor of Electrical and Computer Engineering, NJIT

Dr. Alexander M. Haimovich, Committee Member   Date
Professor of Electrical and Computer Engineering, NJIT

Dr. Osvaldo Simeone, Committee Member   Date
Assistant Professor of Electrical and Computer Engineering, NJIT

BIOGRAPHICAL SKETCH

Author: Alex Ruiz Lee

Degree: Master of Science in Telecommunications

Date: January 2008

Undergraduate and Graduate Education:

- Master of Science in Telecommunications,
  New Jersey Institute of Technology, Newark, NJ, 2008

- Bachelor of Science in Business Administration,
  University of Barcelona, Barcelona, Spain, 2007

- Master of Science in Electronics,
  Technical University of Catalonia, Barcelona, Spain, 2006

- Bachelor of Science in Telecommunications,
  Technical University of Catalonia, Barcelona, Spain, 2004

Major: Telecommunications

To Jeimy, my parents José and So-Kyung and my brother Pepín

ACKNOWLEDGMENT

I would like to thank my academic advisor, Prof. Yeheskel Bar-Ness, for giving me the opportunity to complete my studies at NJIT and let me be part of the Center for Wireless Communications and Signal Processing Research. One of my dreams since I was a child had been to come to the United States to study, and thanks to him my dream has come true. I will always be grateful.

A lot of gratitude for Dr. Alexander Haimovich for accepting to be a member of the defense committee.

Very special thanks go to Dr. Osvaldo Simeone, not only for being part of my defense committee, but for being my mentor during this last stage at NJIT. Just when I thought I was completely lost, you guided me towards the right direction.

I must not forget to acknowledge Igor Stanojev, whose experience has helped me from the very first day. Thanks for being there always when I needed advice or a friend at the lab.

How could I forget Marlene Toeroek, who has been always there to help me.

I would like to give a special thanks to Elisa Sayrol and Eduard Alarcón, current Dean and Vice Dean of International Affairs of the Telecommunication Engineering School at UPC, for choosing me as one of the students that could have the privilege to come to NJIT to complete their studies.

Thanks to Toni Betrán, Pete Hagan and Alexander Medina for everything you have done for me during these three semesters and especially for being my best buddies at NJIT. Thanks to you all, I will remember my days at NJIT as some of the best days of my life.

I would like to thank also my best friends from Barcelona: Jordi Díaz López, Xavier López Prieto, Ignacio Mellado Bataller, Luis Oller Ibars and Carlos Otón Beltrà. Without your support, friendship and class notes I would not be here right now. Thank you all.

There are no words to describe how grateful I am to my family. Thanks for all your support and love. I owe you everything in this world.

Finally, I would like to thank Jeimy, the love of my life. Thanks for your unconditional support, for your love and especially thanks for letting me share my life with you. I love you more than words can say.

TABLE OF CONTENTS

TABLE OF CONTENTS
(Continued)

LIST OF TABLES

LIST OF FIGURES

Figure   **Page**

CHAPTER 1

INTRODUCTION

Wireless communication market is growing rapidly, especially within the last 15 years, during which wireless communication devices have become more and more popular. This growth does not seem to have a stop in the near future as the public keeps demanding more sophisticated devices capable of provide them with voice and data services at higher rates. WiMax technology has been developed as a solution for broadband access networks to cover this need for high voice and date rates, and our work presented here is focused on this technology. In particular, we consider the problem of designing retransmission protocols for a fast moving network, e.g., a train, while it is connected to a WiMax infrastructure, through base stations located along the path, as sketched in Fig. 1.1, which provides data services to terminals therein. Due to its simplicity of the equalization process for multicarrier signals [1], we focus on an OFDM-based radio interface as modulation scheme. Specified reliability requirements in terms of data packet delivery can be guaranteed through Hybrid Automatic Retransmission reQuest (HARQ) protocols (e.g., [1] for application to WiMax systems). In the presence of moving networks with OFDM, the problem of packet loss and the need for HARQ techniques is emphasized by the performance degradation at the physical layer due to Doppler spread, which causes a loss of subchannel orthogonality resulted from interchannel interference (ICI). Finally, with high speed receivers, the implementation of retransmission (HARQ) protocols is inevitably linked with the problem of devising adequate handover strategies from one base station to the following. As an example, retransmission of a given packet might occur after the moving receiver has reached a different area covered by the next base station along the path.

In this work, we compare the performance of different protocols that jointly perform HARQ retransmission and handover. In particular, we consider both hard handover and soft handover via diversity, beamforming and Alamouti's techniques. Performance comparison is based on the evaluation of the average number of retransmissions per packet by numerical simulations. This comparison is presented using two different models. In the first model, the channel is assumed to be frequency nonselective and is simplified by assuming that it changes in a linear fashion during one OFDM symbol period. Furthermore, the SINR at the receiver is used as performance criterion to decide whether a packet is lost or not. The second model considers a frequency selective channel, and uses the BER at the receiver as performance

criterion. Our results point to the importance of a joint design of HARQ and handover, and highlight the relevant performance gains that can be harnessed by means of coordination among successive base stations in the form of beamforming and space-time coding.
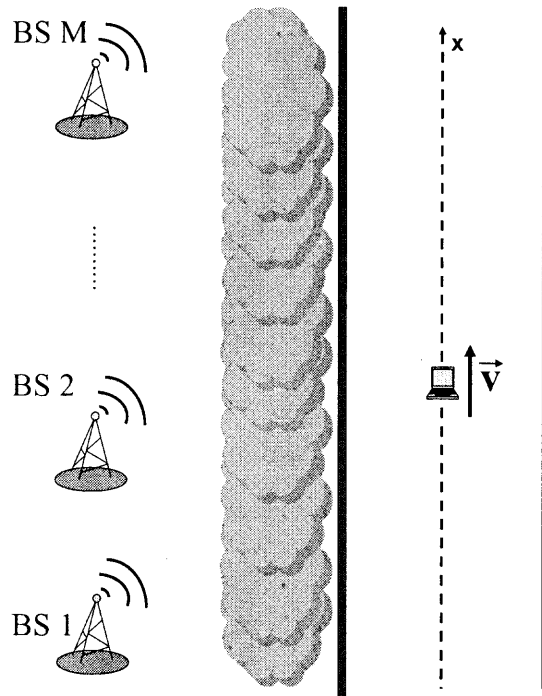
Figure 1.1 Illustration of the scenario of interest

1.1 Orthogonal Frequency Division Multiplexing (OFDM)

The basic idea of OFDM is to split a high rate data stream into a number of lower rate streams as shown in Figure 1.2 and transmit these streams simultaneously, and in parallel over a number of orthogonal subcarriers. The orthogonality of subcarriers guarantees that the streams do not interfere with one another. A general block diagram of an OFDM system is shown in Figure 1.3.

Each data stream is sent in one subchannel, so that each has its own coherence bandwidth. If the bandwidth of transmitted signal is less than coherence bandwidth of the channel, inter-symbol interference (ISI) is eliminated on that channel. Lower data rate streams have lower bandwidth and therefore, if we choose enough subcarriers, we will be able to have very low-rate parallel data streams in each such that each subchannel will be ISI free.
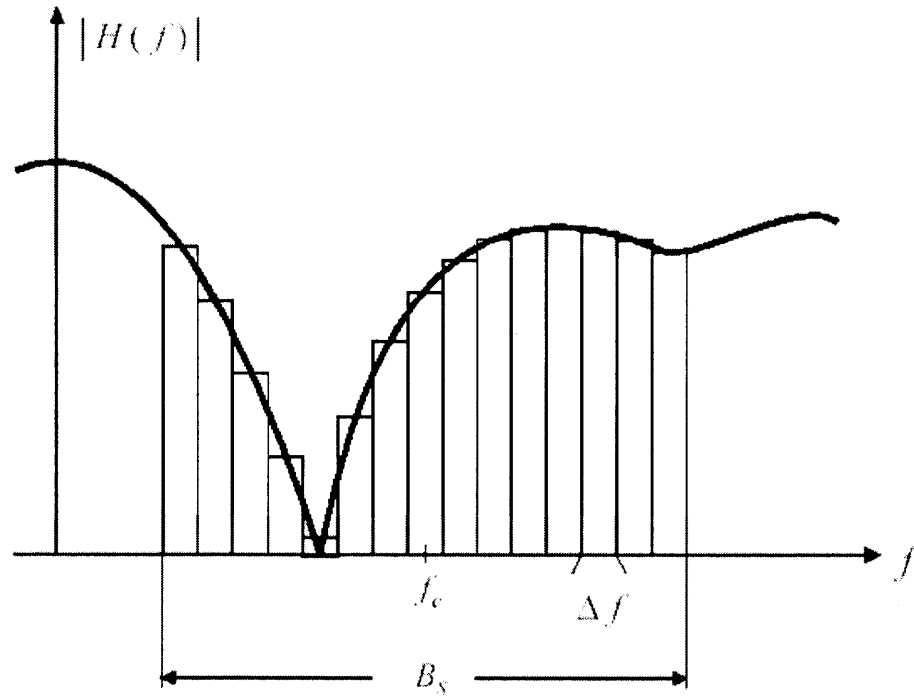
Figure 1.2 Subcarrier division on an OFDM system

The number of bits assigned to each sub-carrier is variable based on the variability of signal to noise ratio (SNR) across the frequency range. The number of sub-carriers, N, used in an OFDM system is chosen as a trade-off between the frequency offset of adjacent carriers and the adjacent channel interference. A greater number of sub-carriers implies less adjacent channel interference, but increased susceptibility to frequency offset, and viceversa.

1.1.1 OFDM and Orthogonality Concept

The division of data stream to several sub-carriers can be implemented easily using Inverse Fast Fourier Transform (IFFT). The match filtering of each sub-channel also is done by Fast Fourier transform (FFT). These operations perform reversible linear mappings between N complex data symbols and N complex OFDM symbols. An N-point FFT requires only on the order of $NlogN$ multiplications rather than N^2 as in a straightforward computation. Due to this fact, an OFDM system typically requires fewer computations per unit time than an equivalent system with equalization. In OFDM the sub-carrier pulse used for transmission is chosen to be rectangular. This has the advantage that a simple Inverse Discrete Fourier Transform (IDFT), which can be implemented very efficiently as Inverse Fast Fourier Transform (IFFT),
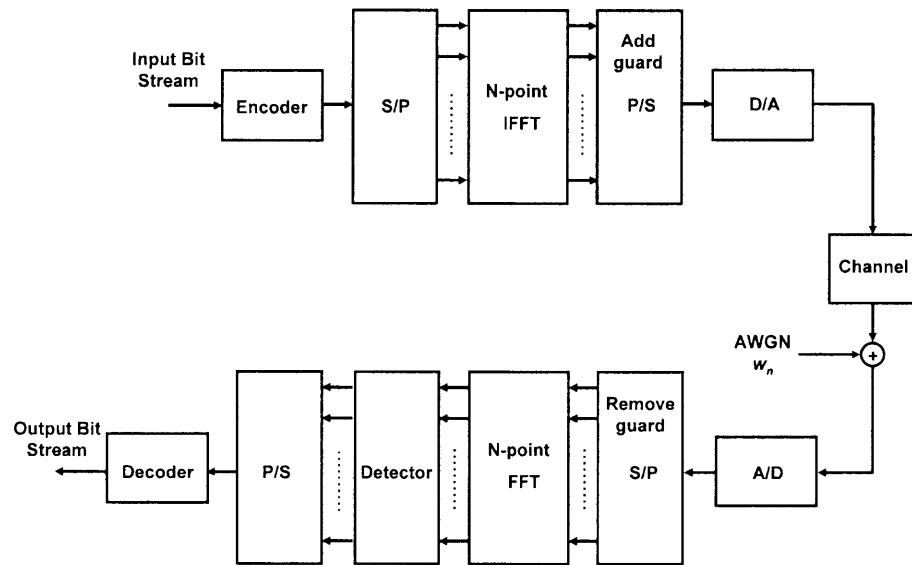
Figure 1.3 Baseband block diagram of an OFDM system

can perform the task of pulse forming and modulation. Accordingly, in the receiver we only need a FFT to reverse this operation. According to the theorems of the Fourier Transform the rectangular pulse shape will lead to a $\sin x / x$ type of spectrum of the sub-carriers as it is shown in Figure 1.4.
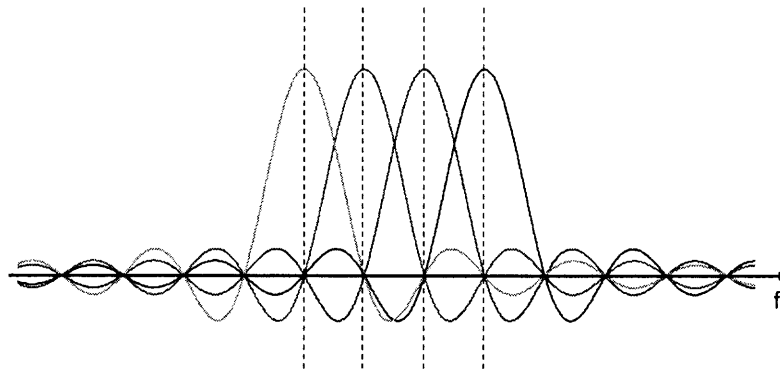
Figure 1.4 OFDM and orthogonality principle

Obviously the spectrums of the sub-carriers are not separated but overlapped. The reason why the information transmitted over the carriers can still be separated is the socalled orthogonality relation. By

using an IFFT for modulation we implicitly choose the spacing of the sub-carriers in such a way that at the frequency where we evaluate the received signal (indicated as dotted lines) all other signals are zero.

Transmission of data in the frequency domain using an FFT, as a computationally efficient orthogonal linear transformation, results in robustness against ISI in the time domain.

1.1.2 OFDM System in Non-ideal Channel Conditions

In real mobile radio environments, transmitted signals are usually subjected to time or frequency dispersion which causes unacceptable error performance degradation. This degradation is known as intersymbol interference (ISI) when it is introduced by the frequency selectivity of the channel or interchannel interference (ICI) when it is introduced by the time selectivity of the channel.

The first problem of ISI can be solved by creating a cyclically extended guard interval time in each OFDM symbol, where each OFDM symbol is preceded by a periodic extension of the signal itself. The total symbol duration is then

$$T_{total} = T_g + T_s, \tag{1.1}$$

where T_g is the guard interval time and T_s is the OFDM symbol time. Figure 1.5 shows a typical guard interval insertion. Each symbol is made of two parts. The whole signal is contained in the active symbol, the last part of which is also repeated at the start of the symbol and is called guard interval. The reason for this is to convert the linear convolution of the signal and channel to a circular convolution and thereby causing the DFT of the circularly convolved signal and channel to simply be the product of their respective DFTs. If the guard interval time is longer than the multipath delay of channel, the effect of ISI can be eliminated. The ratio of the guard interval to the useful symbol duration is applicationdependant because the insertion of guard interval will reduce the data throughput. At the receiver-end this guard interval should be removed before taking FFT from the received signal.

For simplicity, in this work, we always assume that the guard interval time is longer than the multipath delay of the channel, and therefore it eliminates perfectly the ISI.

When the channel is time variant and the channel characteristics change over the duration of one OFDM symbol duration, subcarriers lose their orthogonality. These changes can be modeled by a Doppler spread caused by the relative motion between the receiver and the transmitter. This loss of orthogonality reduces slightly the useful signal in each subcarrier, and introduces interchannel interference (ICI),

Symbol M-1	Guard interval	Symbol M		Guard interval	Symbol M+1
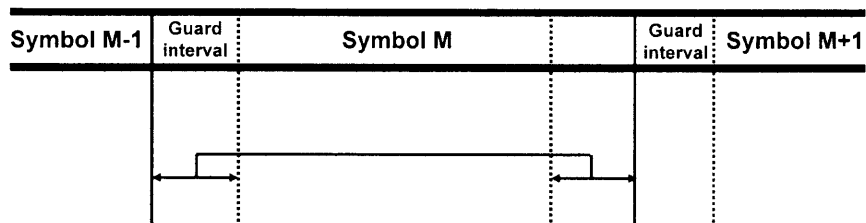
Figure 1.5 Guard interval insertion

leading to a reduction in the effective SINR. Furthermore, the performance degration due to ICI becomes significant as the carrier frequency, block size and receiver speed increase. This performance degration due to time selectivity of the channel has been studied in [2] - [6].

CHAPTER 2

SYSTEM MODEL

The scenario of interest consists of one receiver traveling at a given speed v while connected to a wireless network through M active base stations located along the path. As shown in Fig. 2.1, the base stations are located at a fixed distance R from the path followed by the receiver and at a distance d from each other, starting at $x = 0$. Moreover, OFDM is assumed to be employed as radio interface as in, e.g., WiMax networks. A HARQ retransmission protocol is considered, so that packets that are not received correctly by the moving terminal are retransmitted until successful reception or until a maximum number of retransmissions L is reached. In particular, we assume type-I HARQ, whereby the receiver simply discards previously received copies of a packet and decodes based on the last received copy. It is noted that extension of the analysis to more advanced HARQ protocols such as Chase Combining [7] is conceptually straightforward. Finally, the fading channels between base stations and receiver are assumed to be Ricean distributed in order to account for a line-of-sight component.
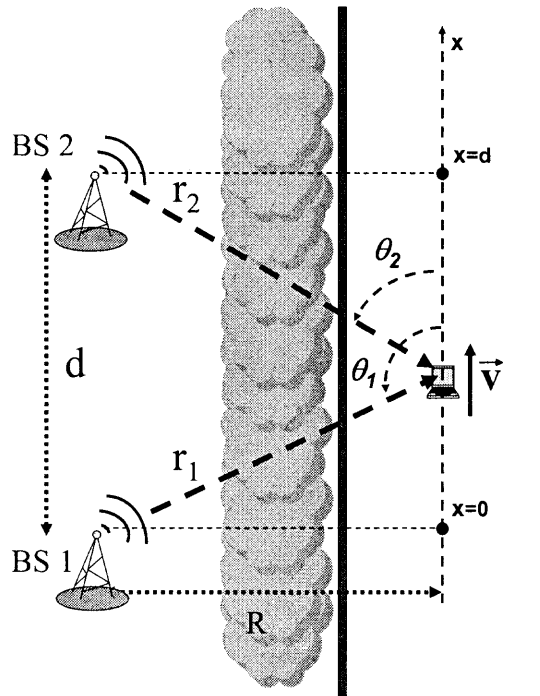
Figure 2.1 Detailed illustration of the scenario of interest with M=2 active base stations

In the described scenario, communication from the base stations to the moving receiver has to deal with two main issues:

- The speed of the receiver causes a *Doppler shift* f_d (in Hz) on the line-of-sight component that produces a loss of subchannel orthogonality as a result of interchannel interference (ICI) and hence higher packet loss [2];

- Movement of the receiver introduces the need for handover, that is the switching the active communication session from one base station to the next.

Because of the relevant Doppler shift, and corresponding ICI, we consider scenarios with relatively large number of retransmissions per packet (large probability of block error). Moreover, due to the movement of the receiver, it is generally advantageous to enable handover even within the same HARQ session, that is to allow successive copies of a given packet to be transmitted by a different base station. Finally, we remark that, besides hard handover schemes, in the scenario at hand transmit spatial diversity (soft handover) can be leveraged.

CHAPTER 3

SNR-BASED MODEL FOR FREQUENCY NON-SELECTIVE CHANNELS

In this chapter, we present a simplified model by assuming that the channel is frequency non-selective and relying on the results obtained in [2], where the BER performance of an OFDM system over time-varying frequency non-selective fast Ricean channels is analized using an approximation of the channel variations by a linear model, as proposed in [3].

We are interested in obtaining an analitical closed expression for the instantaneous Signal-to-Interference-plus-Noise ratio (SINR) at the receiver, accounting for both additive noise and ICI, which will be used as performance criterion to determine whether a packet is lost or not. A packet will be considered to be successfully received if the instantaneous Signal-to-Interference-plus-Noise ratio (SINR), accounting for both additive noise and ICI, at the receiver is above a threshold γ. According to the HARQ protocol, retransmission of an erroneously decoded packet is performed after a time τ seconds, which in practice depends on the specific implemented retransmission protocol and on the round trip signaling times.

3.1   Signal Model

We consider an OFDM system with N subcarriers, an input data symbols sequence $(X_0, X_1, \ldots, X_{N-1})$ corresponding to subcarriers $0, 1, \ldots, N-1$ and bandwidth $1/T_s$, where T_s is the symbol period.

With reference to Figure 1.3, an input data bits are first encoded into symbols (X_m), and then the Serial-to-Parallel converter (S/P) transmits N symbols to the OFDM modulator (N-point IFFT block), where each symbol is modulated by the corresponding subcarrier as:

$$x_n = \sum_{m=0}^{N-1} X_m e^{j2\pi nm/N}, \tag{3.1}$$

where x_n represents the nth sample of the output of the IFFT. After this, the guard interval is inserted in each OFDM symbol to avoid ISI and to preserve the orthogonality of the subchannels. Each OFDM symbol is then sampled and D/A converted and finally sent through a multipath fading channel consisting

of L discrete paths. At the receiver, after the signal has been A/D converted and the guard interval has been removed, the received signal from M active base stations at time n can be written as:

$$y_n = \sum_{i=1}^{M} \sum_{l=0}^{L-1} \delta_i h_{n,l,i} x_{n-l,i} + w_n, \tag{3.2}$$

where: subscript i denotes different base stations, δ_i accounts for the path loss and is equal to $(R/r_i)^{\eta/2}$ with r_i being the distance between base station i and receiver and η is the path loss exponent which depends on the specific propagation environment (Table A.1 in Appendix A); $h_{n,l,i}$ is a nonzero mean complex Gaussian variable accounting for the channel response for the lth path; $x_{n,l,i}$ is the nth time-sample of the trasmitted sequence from base station i for the lth path; and w_n is additive white Gaussian noise (AWGN) with power N_0.

Assuming time-varying flat fading channel, i.e., no multipath is considered, the received signal in (3.2) can be simplified as follows:

$$y_n = \sum_{i=1}^{M} \delta_i h_{n,i} x_{n,i} + w_n. \tag{3.3}$$

If we further assume that the phase shift caused by the fading channel can be recovered perfectly (as assumed in e.g., [2] [3]) and compensated individually for each time sample, the received signal in (3.3) can be written as:

$$y_n = \sum_{i=1}^{M} \delta_i |h_{n,i}| x_{n,i} + w_n, \tag{3.4}$$

where $|h_{n,i}|$ is the channel gain amplitude taken as Ricean random variable with Ricean factor K and power $\xi = E[|h_{n,i}|^2] = 1 \ \forall n, i$.

At the receiver, the demodulated signal on subcarrier k, Y_k, is obtained by taking the FFT of the received sequence y_n, leading to

$$\begin{aligned} Y_k &= \sum_{i=1}^{M} \left[\delta_i \sum_{m=0}^{N-1} H_{k-m,i} X_{m,i} \right] + W_k \\ &= \sum_{i=1}^{M} \left[\delta_i H_{0,i} X_{k,i} + \delta_i \sum_{m=0, m \neq k}^{N-1} H_{k-m,i} X_{m,i} \right] + W_k, \end{aligned} \tag{3.5}$$

where W_k denotes the FFT of noise w_n and $H_{k,i}$ is the FFT of the time-variant Ricean flat fading channel $|h_{n,i}|$ as follows:

$$H_{k,i} = \frac{1}{N} \sum_{n=0}^{N-1} |h_{n,i}| e^{-j2\pi nk/N}. \tag{3.6}$$

Substituing equation (3.6) into (3.5) we get:

$$
\begin{aligned}
Y_k &= \sum_{i=1}^{M} \left[\delta_i \left(\frac{1}{N} \sum_{n=0}^{N-1} |h_{n,i}| \right) X_{k,i} \right. \\
&\quad \left. + \delta_i \left(\frac{1}{N} \sum_{m=0,m\neq k}^{N-1} \sum_{n=0}^{N-1} |h_{n,i}| e^{-j2\pi n(k-m)/N} X_{m,i} \right) \right] \\
&\quad + W_k \\
&= \sum_{i=1}^{M} [\delta_i \alpha_i X_{k,i} + \delta_i \beta_{k,i}] + W_k, \tag{3.7}
\end{aligned}
$$

where

$$\alpha_i = \frac{1}{N} \sum_{n=0}^{N-1} |h_{n,i}| \tag{3.8}$$

represents the multiplicative distortion at the desired subchannel and

$$\beta_{k,i} = \frac{1}{N} \sum_{m=0,m\neq k}^{N-1} \sum_{n=0}^{N-1} |h_{n,i}| X_{m,i} e^{-j2\pi n(k-m)/N} \tag{3.9}$$

represents the ICI. Notice that, if the channel is considered to be time-invariant during a block period, $\beta_{k,i}$ vanishes, implying that no ICI exists. As mentioned previously, $|h_{n,i}|$ is considered to be time-variant and thus ICI exists. However, a remarkable simplification can be reached taking the assumption that the channel varies in a linear fashion during one OFDM symbol. This assumption was first taken in [3] and then applied in [2] to analyse the BER perfomance of an OFDM system over frequency nonselective Ricean fading channels. Relying on those analysis, the equivalent channel gain α_i in (3.7) can be aproximated as:

$$\alpha_i = \frac{1}{2}(|h_{0,i}| + |h_{N-1,i}|) \tag{3.10}$$

and its probability density function can be represented as in [2]:

$$f_{\alpha_i}(\rho) = \tag{3.11}$$

$$2 \int_0^{2\rho} \frac{(1+K)^2(2\rho - y)y}{2\pi\xi^2(1 - \mu_i^2)}$$

$$\exp\left[\left(\frac{-2K}{1+\mu_i}\right) - \frac{(1+K)[(2\rho - y)^2] + y^2}{2(1 - \mu_i^2)\xi}\right]$$

$$\int_0^{2\pi} \exp\left[\frac{\mu_i(1+K)(2\rho - y)y\cos\theta}{(1 - \mu_i^2)\xi}\right]$$

$$I_0\left(\sqrt{\frac{2K(1+K)\left[(2\rho - y)^2 + y^2 + 2(2\rho - y)y\cos\theta\right]}{\xi(1+\mu_i)^2}}\right)$$

$$d\theta dy, \rho \geq 0,$$

where μ_i is defined as:

$$\mu_i = J_0\left(2\pi f_{d_i} T_s(N-1)\right), \tag{3.12}$$

with f_{d_i} being the *Doppler shift* f_{d_i} suffered by the signal transmitted from base station i and is given by [8]:

$$f_{d_i} = \frac{v}{\lambda}\cos\theta_i, \tag{3.13}$$

where v is the speed of the receiver, λ is the wavelenght of the frequency carrier and θ_i is the angle between the direction of the motion of the receiver and the direction of arrival of the signal (as illustrated in Fig. 2.1).

Figures 3.1 and 3.2 show the Probability Density Function (PDF) and the Cumulative Distribution Function (CDF) of α_i respectively, for different values of θ_i from $\theta_i = 137°$ to $\theta_i = 165°$ at a fixed speed of $v = 210$ km/h. Furthermore, for this simulation we set $N = 1024$ OFDM subcarriers. The carrier frequency f_c is assumed to be $f_c = 2$ GHz and the symbol period T_s is 7.8125 μs. The Ricean factor K is assumed to be $K = 0$ and $K = 10$ dB. Notice that for $K = 0$, the pdf in (3.11) becomes the pdf of two correlated Rayleigh distributed random variables.

Furthermore, the power of the ICI component $\beta_{k,i}$ can be derived as $\sigma_{\beta_i}{}^2 = E[|\beta_{k,i}|^2]$ [4]:

$$\sigma_{\beta_i}{}^2 = E_i - \frac{E_i}{N^2}\left(N + 2\sum_{j=1}^{N-1}(N-j)J_0(2\pi f_{d_i} T_s j)\right), \tag{3.14}$$
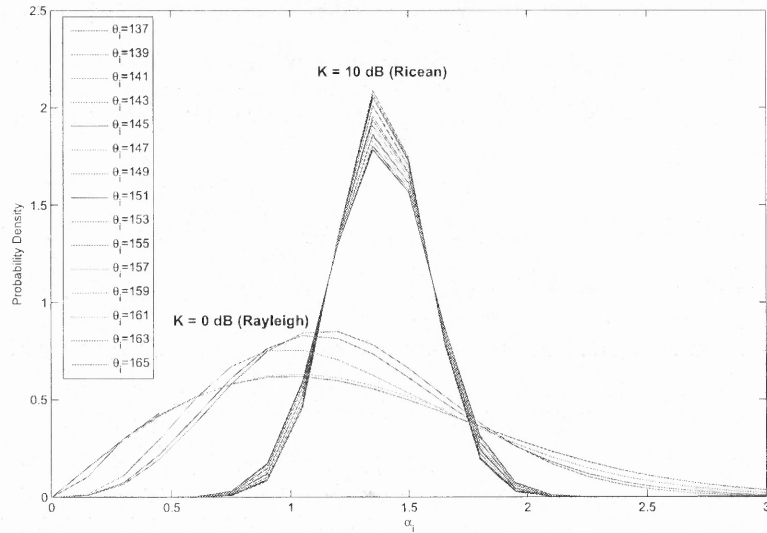
Figure 3.1 PDF of α_i for $v = 210$ km/h, $\theta_i \in [137°, 165°]$ and K=0,10 dB

where we define $E_i = E[|X_{k,i}|^2]$ as the per-symbol energy transmitted from base station i. Noticing that the ICI power $\sigma_{\beta_i}^2$ are the same for each subcarrier [2], we can omit subscript k in the following.

3.2   Retransmission Protocols

In this section we describe five different protocols which jointly perform HARQ retransmission and handover. The relative merits of these techniques will be then discussed in section IV via numerical results. It should be noted that while the first two protocols are based on hard handover, the latter three exploit soft handover (spatial diversity).

3.2.1   Protocol 1

This protocol combines HARQ with hard handover between adjacent base stations. Just one base station transmits at any given time and handover is performed once the receiver approaches the next base station, even within the same HARQ session corresponding to the transmission of a given packet. The corresponding areas of coverage of different base stations are as indicated in Fig. 3.3, where for simplicity of notation, and henceforth, we refer to base stations 1 and 2.
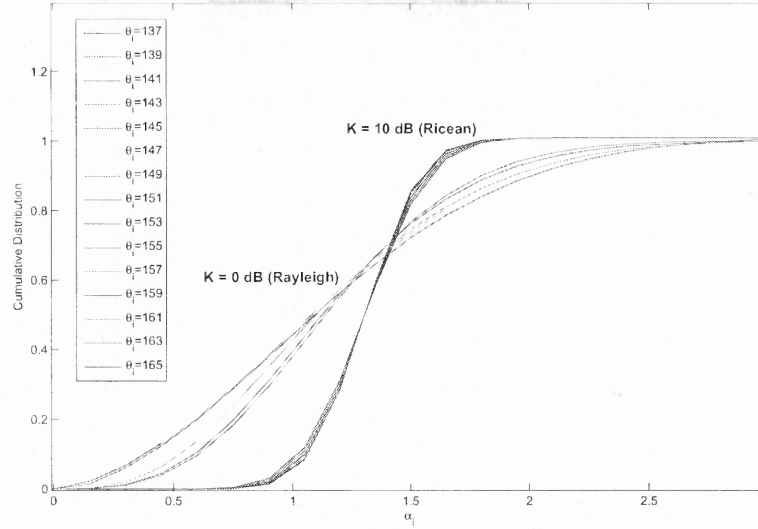
Figure 3.2 CDF of α_i for $v = 210$ km/h, $\theta_i \in [137°, 165°]$ and K=0,10 dB

In this case, since only one base station trasmits at a given time, equation (3.7) can be simplified as:

$$Y_k = \delta_i \alpha_i X_k + \delta_i \beta_{k,i} + W_k, \tag{3.15}$$

where i could be either 1 or 2 depending on which base station is transmitting in the active HARQ session. From equation (3.15) the instantaneous SINR can be written as:

$$SINR = \frac{\delta_i^2 \alpha_i^2 E_i}{\delta_i^2 \sigma_{\beta_i}^2 + N_0/2} \qquad i = 1, 2 \tag{3.16}$$

where both base stations transmit the same power, namely, $E_1 = E_2 = E_s$.

3.2.2 Protocol 2

This second protocol also combines HARQ with hard handover between adjacent base stations, but in this case the handover is performed once the receiver approaches half the distance between base stations, so that the areas of coverage are as indicated in Fig. 3.5.

Since the only difference with the previous protocol is the area of coverage of each base station, the instantaneous SINR at the receiver can be expressed as in equation (3.16).
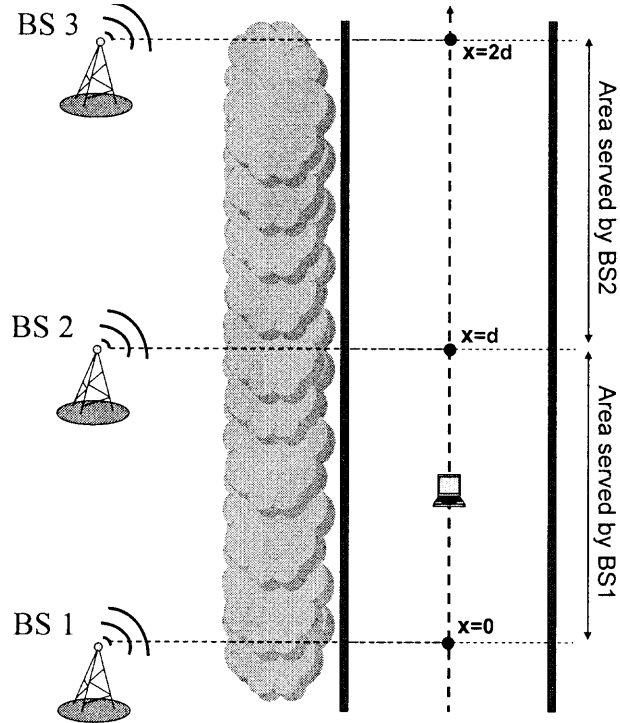
Figure 3.3 Area of coverage of adjacent base stations for protocol 1.

3.2.3 Protocol 3: Selection Diversity

According to this third protocol, the two base stations nearest the receiver transmit simultaneously the same sequence, $x_{n,1} = x_{n,2} = x_n$, on two orthogonal spectral resources for any packet (as in FDMA or TDMA). The receiver compares the SINR of both signals and chooses the signal with largest SINR. In order to maintain the same overall transmission energy per packet, we assume that each base station transmits with half power with respect to protocols 1 and 2, i.e., $E_1 = E_2 = E_s/2$. Notice, however, that this protocol is more expensive in terms of bandwidth as compared to protocols 1 and 2 due to the requirement on orthogonal transmissions. It follows that the equivalent SINR at the receiver is:

$$SINR = \max\{SINR_1, SINR_2\}, \tag{3.17}$$

where $SINR_1$ and $SINR_2$ are the SINRs of the signal received from base station 1 and base station 2 respectively and are expressed as in equation (3.16).

(a)   **(b)**

Figure 3.4 Protocol 1: the receiver is served by BS1 when it is located at $x \in [0, d)$ (a), and by BS2 when it is located at $x \in [d, 2d)$

3.2.4 Protocol 4: Beamforming

This protocol exploits beamforming to control the directionality of the transmission in order to enhance the received SINR. This technique consists in applying weighting factors w_i to the signal of interest $x_{n,i}$ at the base stations, so the transmitted signal from base station i is:

$$x_{n,i}\prime = w_i x_{n,i} \quad i = 1, ..., M \tag{3.18}$$

where M is the number of active base stations and w_i are the weighting factors satisfying

$$\sum_{i=1}^{M} |w_i|^2 = 1. \tag{3.19}$$

The above constraint ensures that the transmitted power is not being increased. This technique is called transmit beamforming because the signal $x_{n,i}$ is being formed before being transmitted. In this protocol, the two base stations nearest to the receiver, BS1 and BS2 transmit simultaneously the following signals:

$$x_{n,1}\prime = \frac{h_{n,1}^*}{|h_{n,1}|} x_n \tag{3.20}$$
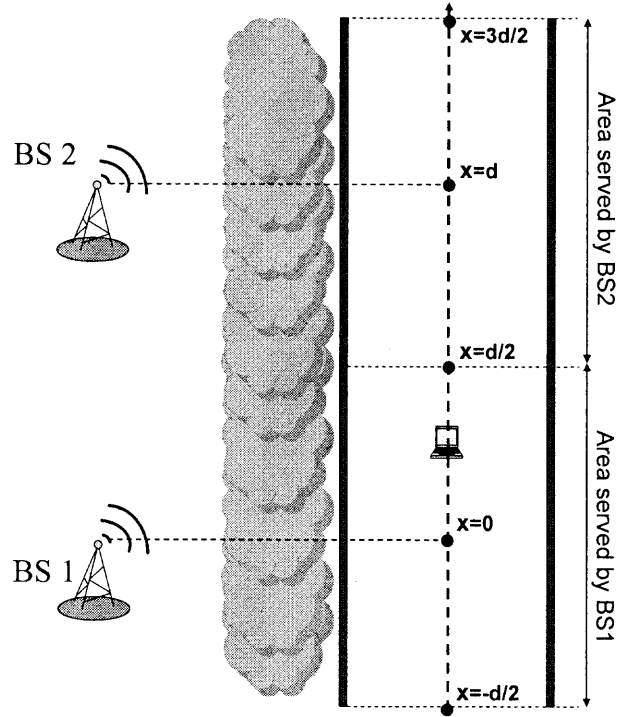
$$x_{n,2}\prime = \frac{h_{n,2}^*}{|h_{n,2}|} x_n$$

Figure 3.5 Area of coverage of adjacent base stations for protocol 2.

where $(h^*_{n,1}/|h_{n,1}|)$ and $(h^*_{n,2}/|h_{n,2}|)$ are the weighting factors (satisfying constraint (3.19)). Notice that, unlike protocol 3, the two nearest base stations transmit simultaneously on the same spectral resource for any packet.

Recalling (3.3) the received signal can be written as:

$$y_n = \delta_1 \frac{h^*_{n,1} h_{n,1}}{|h_{n,1}|} x_n + \delta_2 \frac{h^*_{n,2} h_{n,2}}{|h_{n,2}|} x_n + w_n$$

$$= \delta_1 |h_{n,1}| x_n + \delta_2 |h_{n,2}| x_n + w_n. \tag{3.21}$$

Notice that, unlike the previous protocols, the channel phase does not need to be known at the receiver, since the phase is already compensated through the operation $(h^*_{n,i} h_{n,i}/|h_{n,i}|) = |h_{n,i}|$. Taking the FFT of the received sequence and following the same steps as in equations (3.5) through (3.7), the demodulated signal on subcarrier k can be proved to be:

$$Y_k = (\delta_1 \alpha_1 + \delta_2 \alpha_2) X_k + \delta_1 \beta_{k,1} + \delta_2 \beta_{k,2} + W_k, \tag{3.22}$$

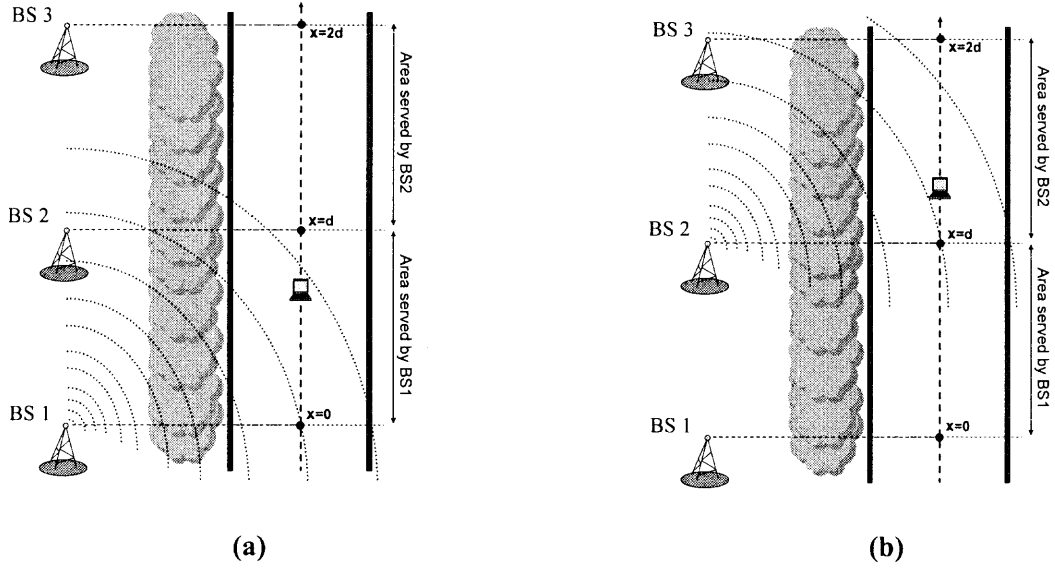(a)   (b)
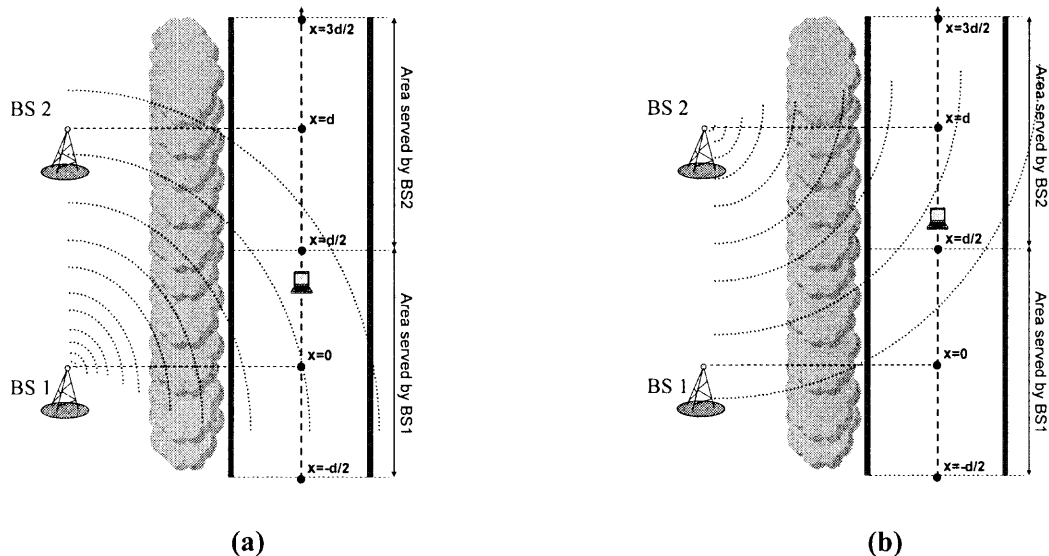
Figure 3.6 Protocol 2: the receiver is served by BS1 when it is located at $x \in [-d/2, d/2]$ (a), and by BS2 when it is located at $x \in [d/2, 3d/2]$

where $\beta_{k,1}$ and $\beta_{k,2}$ are the ICI components for channel 1 and 2 respectively. Assuming that, like protocol 3, each base station transmits at half power with respect to protocols 1 and 2, the received SINR can be then written as:

$$SINR = \frac{(\delta_1 \alpha_1 + \delta_2 \alpha_2)^2 E_s/2}{\delta_1^2 \sigma_{\beta_1}^2 + \delta_2^2 \sigma_{\beta_2}^2 + 2\delta_1 \delta_2 E[\beta_{k,1}\beta_{k,2}] + N_0/2}. \tag{3.23}$$

Correlation $E[\beta_{k,1}\beta_{k,2}]$ is affected by the fact that the transmitted signals from both base stations are correlated (recall (3.21)). However, we will show in Appendix A that, due to the structure of the received signal, $E[\beta_{k,1}\beta_{k,2}] = 0$, and therefore the received SINR can be then written as:

$$SINR = \frac{(\delta_1 \alpha_1 + \delta_2 \alpha_2)^2 E_s/2}{\delta_1^2 \sigma_{\beta_1}^2 + \delta_2^2 \sigma_{\beta_2}^2 + N_0/2}. \tag{3.24}$$

Finally, notice that in this protocol, simultaneous transmissions are coordinated by the availability of channel state information at the base stations, i.e, in order to achieve transmit diversity, the base stations must have the CSI. This presents the problem of having the receiver to send it to the base station, reducing so the throughput. In the next section, we present an alternative technique to beamforming, Alamouti's STBC, which does not need to provide the base station with the CSI.
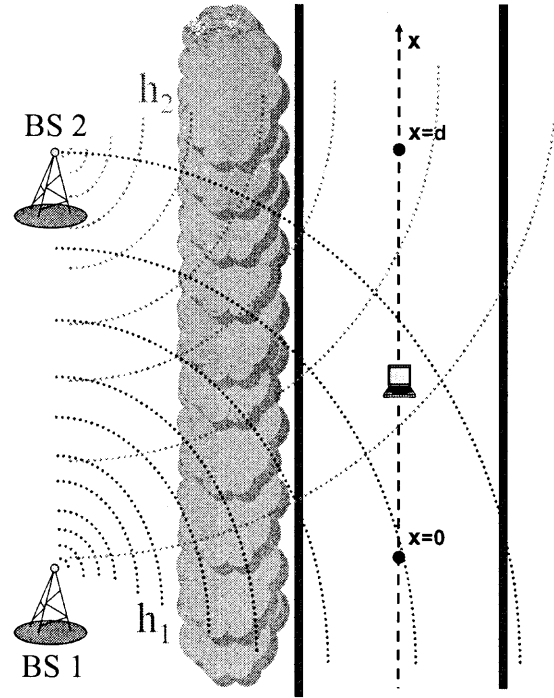
Figure 3.7 Illustration of Protocol 3.

3.2.5 Protocol 5: Alamouti's STBC

This last protocol is based on Alamouti's space-time block coded diversity [9]. Alamouti presented the STBC code that achieves the maximum rate and diversity for two transmitting antennas. According to it and, when applied in the frequency domain, during the first symbol period, $X_{k,1}$ and $X_{k,2}$ are sent from BS1 and BS2 respectively for each $k = 0, 1, ..., N - 1$. During the second symbol period, $-X_{k,2}^*$ and $X_{k,1}^*$ are sent from BS1 and BS2 respectively for each $k = 0, 1, ..., N - 1$. Figure 3.9 illustrates the two base stations transmitting according to this technique. The block diagram of an OFDM system with Alamouti's space-time block coded diversity is shown in Figure 3.10.

Recalling (3.4), at the receiver the received signal from $M = 2$ active base stations at time n can be expressed as:

$$y_{n,p} = \sum_{i=1}^{2} \delta_{i,p} |h_{n,i,p}| x_{n,i,p} + w_{n,p} \quad p = 1, 2 \tag{3.25}$$
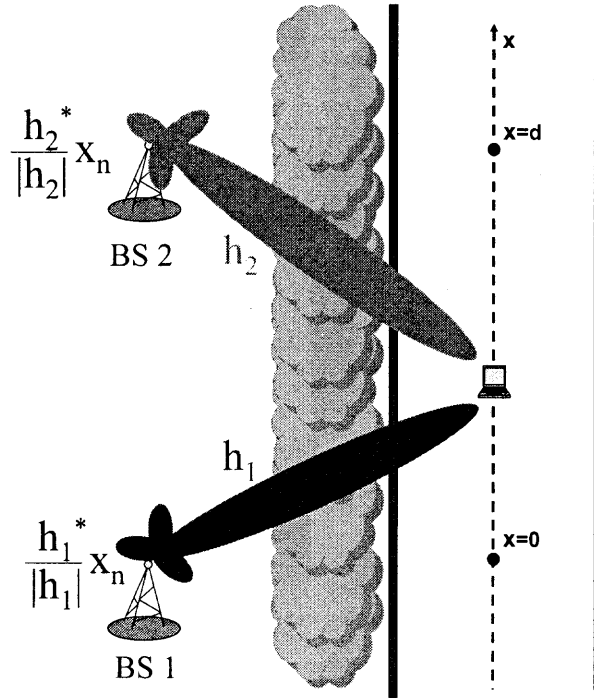
Figure 3.8 Illustration of Protocol 4.

where p denotes the pth symbol period. The modulated signal on subcarrier k after taking the FFT, can be expressed in the frequency domain [10] as:

$$Y_{k,p} = \sum_{i=1}^{2} \sum_{m=0}^{N-1} \delta_{i,p} H_{k-m,i,p} X_{m,i,p} + W_{k,p} \quad p = 1, 2 \tag{3.26}$$

Equation (3.26) can be expressed in matrix notation as [10]:

$$\mathbf{Y}_k = \mathbf{A}_{k,k}\mathbf{X}_k + \sum_{m=0, m \neq k} \mathbf{A}_{k,m}\mathbf{X}_m + \mathbf{W}_k \tag{3.27}$$

where

$$\mathbf{A}_{k,m} = \begin{bmatrix} \delta_{1,1} H_{k-m,1,1} & \delta_{2,1} H_{k-m,2,1} \\ \delta_{2,2} H^*_{k-m,2,2} & -\delta_{1,2} H^*_{k-m,1,2} \end{bmatrix} ; \tag{3.28}$$

$$\mathbf{Y}_k = \begin{bmatrix} Y_{k,1} \\ Y^*_{k,2} \end{bmatrix} ; \quad \mathbf{X}_k = \begin{bmatrix} X_{k,1} \\ X_{k,2} \end{bmatrix} ; \quad \mathbf{W}_k = \begin{bmatrix} W_{k,1} \\ W^*_{k,2} \end{bmatrix} . \tag{3.29}$$
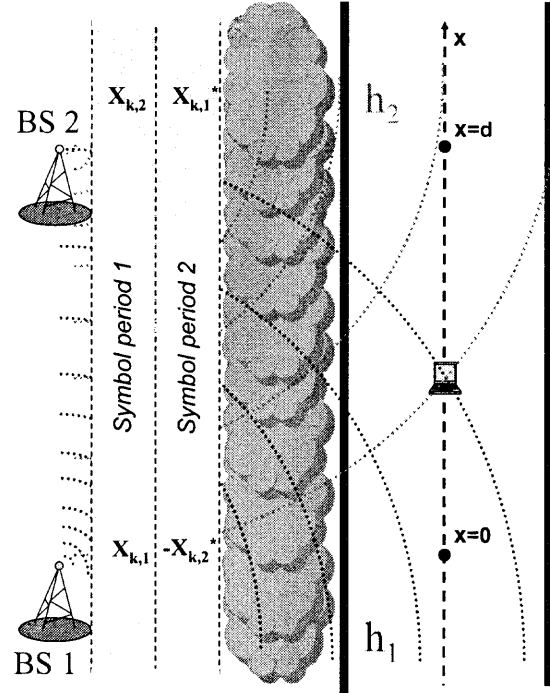
Figure 3.9 Illustration of Protocol 5 with Alamouti's technique applied in the frequency domain

These signals are then combined according to the Alamouti's combining scheme, this is by multiplying the received signal by $\widetilde{\mathbf{A}_k}^H$, being $\widetilde{\mathbf{A}_k}$ defined as:

$$\widetilde{\mathbf{A}_k} = \begin{bmatrix} \alpha_1 & \alpha_2 \\ \alpha_2^* & -\alpha_1^* \end{bmatrix} \tag{3.30}$$

with $\alpha_i \ i = 1,2$ defined in (3.8). Therefore if we define

$$\widetilde{\mathbf{Y}_k} = \widetilde{\mathbf{A}_k}^H \mathbf{Y}_k \tag{3.31}$$

then the received signal after decoding reads

$$\widetilde{\mathbf{Y}_k} = \rho_k \mathbf{I}_2 \mathbf{X}_k + \mathbf{C}_{INTRAk} \mathbf{X}_k + \sum_{m=0,m\neq k} \mathbf{C}_{INTERm} \mathbf{X}_m + \widetilde{\mathbf{W}_k} \tag{3.32}$$

where

$$\rho_k = \alpha_1^2 + \alpha_2^2; \tag{3.33}$$
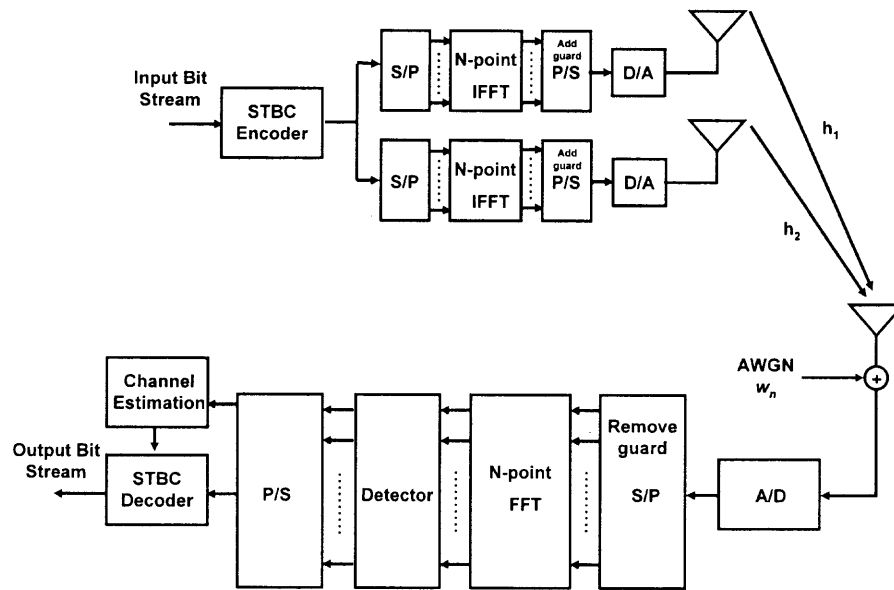
Figure 3.10 OFDM system with Alamouti's space-time block coded diversity

$C_{INTRAk}X_k$ is the intracarrier interference (or intracodeword coupling) that shows the coupling effect between symbols in a codeword with

$$C_{INTRAk} = \widetilde{\mathbf{A}}_k^H \mathbf{A}_{\Delta,k} \tag{3.34}$$

$$\mathbf{A}_{\Delta,k} = \mathbf{A}_{k,k} - \widetilde{\mathbf{A}}_k;$$

$\sum_{m=0,m\neq k} C_{INTERm}X_m$ is the ICI (or intercodeword coupling) that shows the coupling effect between symbols in different codewords with

$$C_{INTERk} = \widetilde{\mathbf{A}}_k^H \mathbf{A}_{k,m} \tag{3.35}$$

and

$$\widetilde{\mathbf{W}}_k = \widetilde{\mathbf{A}}_k^H \mathbf{W}_k. \tag{3.36}$$

An analitical closed expression for the SINR at the receiver can not be written from (3.32), therefore performance of this protocol will not be presented in the numerical results section. However, this protocol will be analized again in the second model presented in this work for frequency selective channels, and numerical results will be then presented.

3.3 Numerical Results

In order to compare the four protocols we consider the averaged number of retransmissions per packet over the fading distribution as the performance criterion, and evaluate it via Monte Carlo simulations. We fix R equals to $R = 5$ m. Moreover, with reference to Fig. 2.1, the receiver travels along the x-axis, and our simulations are focused on HARQ sessions that start within the area between BS1 and BS2. We call x^* or initial position to the point where the HARQ session starts. Figure 3.11 illustrates one HARQ session. Receiver is located at $x = x^*$ when the first transmission of the packet is sent. T retransmissions are needed until the packet is successfully received.
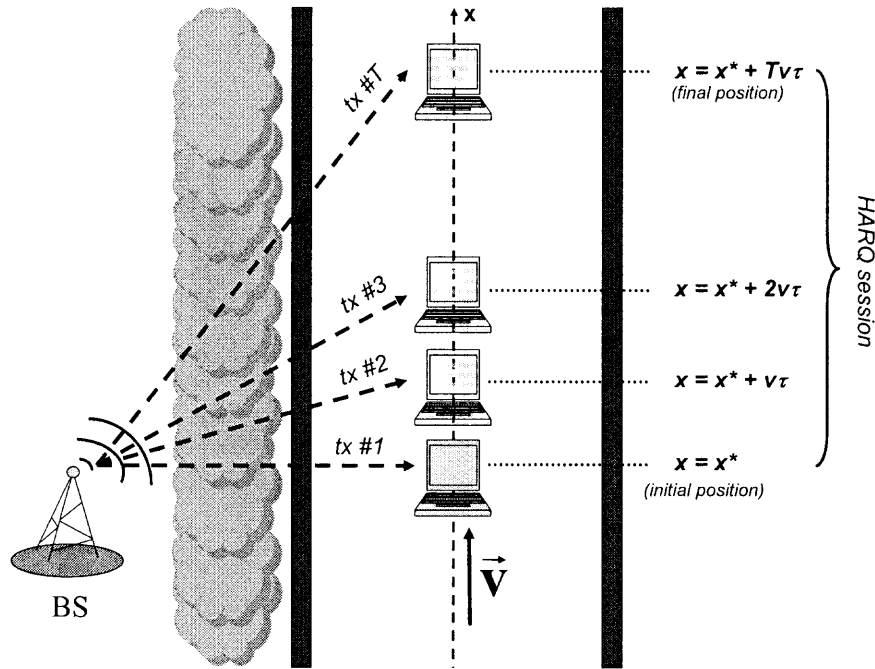
Figure 3.11 Illustration of one HARQ session with x^* being the initial position

A packet is transmitted while the receiver moves, and we are interested in finding the average number of retransmissions necessary for successful transmission. We set $N = 1024$ OFDM subcarriers. The Ricean factor K is assumed to be $K = 10$ dB and $E_s/N_0 = 5$ dB. The carrier frequency f_c is assumed to be $f_c = 2$ GHz and the symbol period T_s is 7.8125 μs. The delay τ between the retransmissions of the same packet has been set to $\tau = 10$ ms. We have considered the path loss exponent η equal to 3 and the threshold γ for the SINR equal to $\gamma = 2$ (3 dB). Finally, the maximum number of retransmissions L is set equal to $L = 25$.

3.3.1 Performance for Fixed Initial Position $x^* = d/2$

Figures 3.12 and 3.13 show the average number of transmissions of the four protocols for two different speeds of the receiver, $v = 60$ and 210 km/h respectively, and for a specific initial position, $x^* = d/2$. As it can be seen, for both speeds beamforming (protocol 4) always presents the lowest rate of transmissions followed by protocol 2 (hard handover according to Fig. 3.5), protocol 3 (selection diversity) and then protocol 1 (hard handover according to Fig. 3.3). Also notice that protocols 2 and 3 require a larger number of retransmissions for $v = 60$ km/h rather than for $v = 210$ km/h. This is due to the fact that when the receiver is located at $x = d/2$ and the transmitted packet gets lost, it is best for the receiver to travel as fast as possible to the second base station in order to experience a better SINR. Finally, it is noted that the number of transmissions tends to the maximum delay $L = 25$ (which implies an outage event) as the distance between base stations d increases.

Figure 3.12 Average number of transmissions per packet for a user starting at $x^* = d/2$ and travelling with velocity v=60 km/h versus distance d between base stations.

3.3.2 Performance for Fixed $d = 20$ m

Figures 3.14 and 3.15 show the performance of the four protocols for the same two different speeds of the receiver but in this case the distance d between base stations has been fixed to $d = 20$ m and the starting
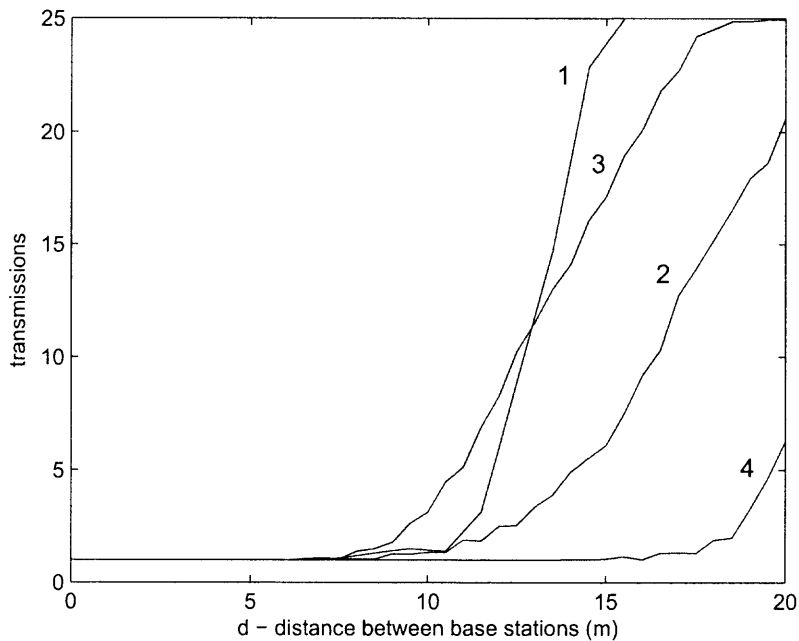
Figure 3.13 Average number of transmissions per packet for a user starting at $x^* = d/2$ and travelling with velocity v=210 km/h versus distance d between base stations.

point x^* varies from $x^* = 0$ to $x^* = 20$ m. For protocol 1, if the starting point x^* is sufficient large, i.e., transmission starts at a large enough distance from the serving base station, successful transmission is not achieved and therefore the maximum number of retransmissions L=25 is reached. This shows the need for a better handover scheme as prescribed by the other protocols. Protocol 2 has increasing number of retransmissions for starting points x^* such that handover to the second base station is not initiated within the HARQ session, and decreasing number of retransmissions after this point. Similarly, protocols 3 and 4 have increasing number of retransmissions for starting points x^* such that the receiver is not able to exploit the signal from the second base station within the given HARQ session due to the small received power, and decreasing number of retransmissions after this point. Accordingly, larger speeds cause the worst-case starting point x^* to become smaller. For instance, in the case of protocol 3 and 4, this is due to the fact the successive retransmissions within the HARQ session benefit from more significant power from the second base station if movements between retransmissions cover larger distances.
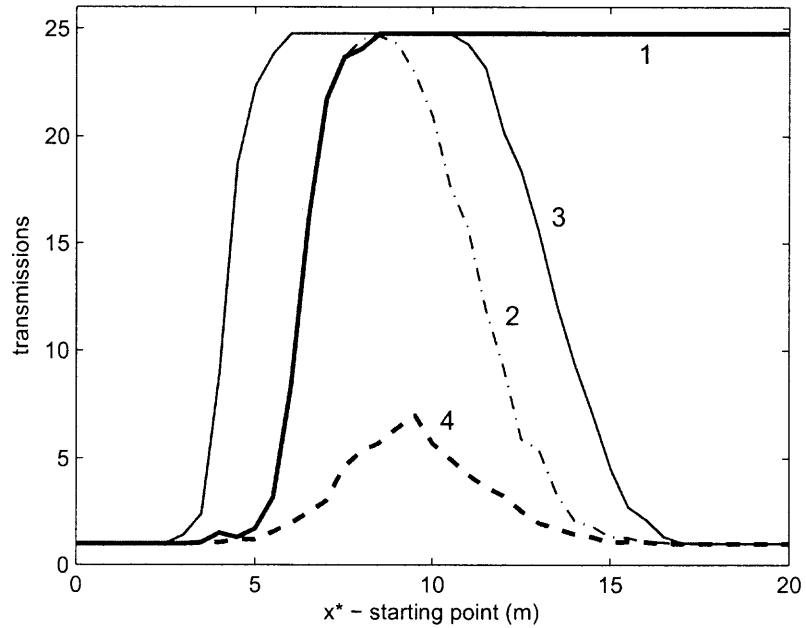
Figure 3.14 Average number of transmissions for distance between base stations $d = 20$ m and travelling with velocity $v=60$ km/h versus starting point x^*.

3.3.3 Performance on Average Over All Initial Positions

As a final evaluation, Figures 3.16 and 3.17 show the number of retransmissions averaged over all initial positions x^* uniformly distributed between 0 and d, versus the distance d between base stations. The basic conclusions drawn above for fixed inital positions are confirmed, namely in terms of the performance comparison between different schemes.
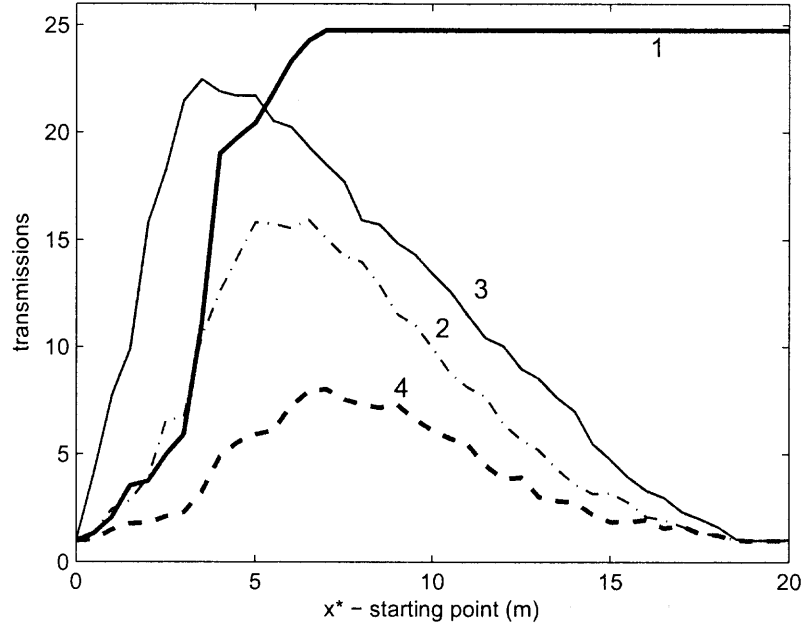
Figure 3.15 Average number of transmissions for distance between base stations $d = 20$ m and travelling with velocity v=210 km/h versus starting point x^*.
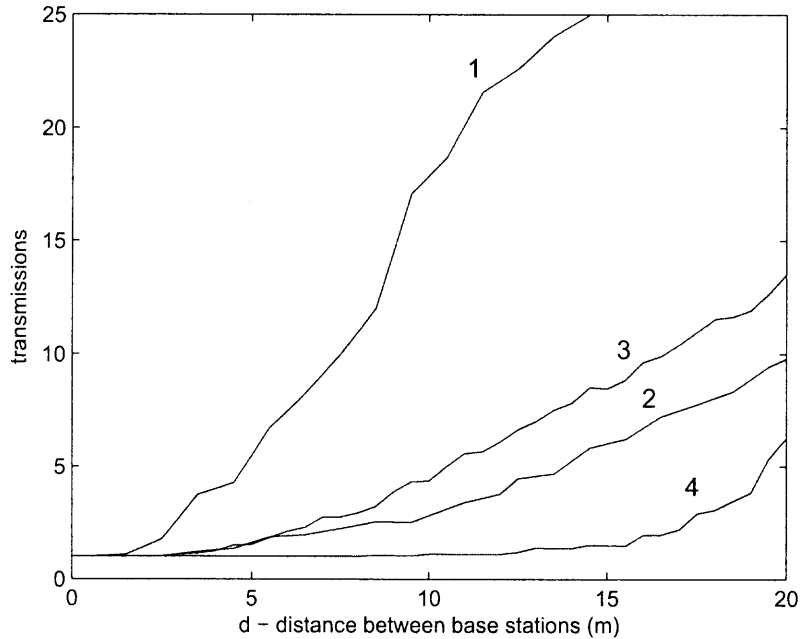

Figure 3.16 Average number of transmissions for starting point $x^* = 0$ and travelling with velocity v=60 km/h versus distance d between base stations.

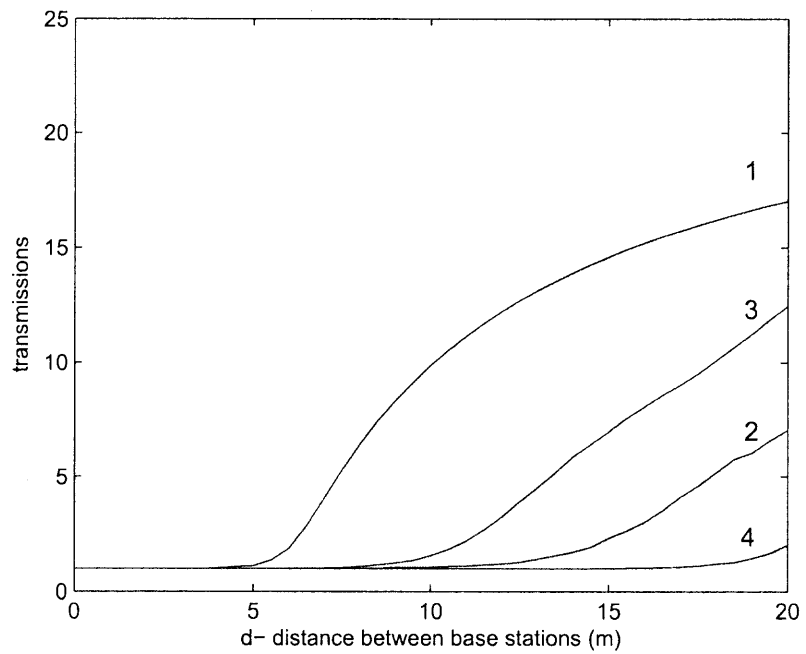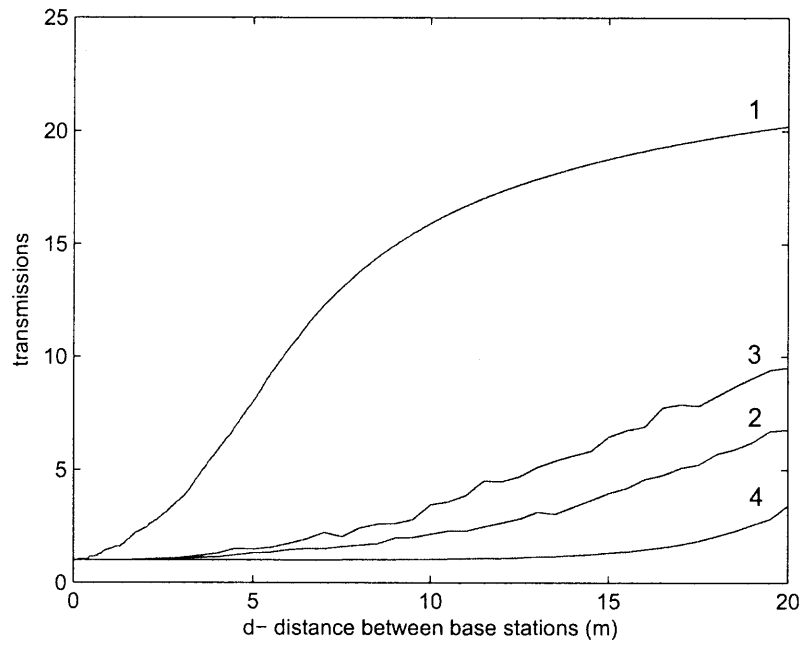**Figure 3.17** Average number of transmissions for starting point $x^* = 0$ and travelling with velocity v=210 km/h versus distance d between base stations.

CHAPTER 4

BER-BASED MODEL FOR FREQUENCY SELECTIVE CHANNELS

In this chapter we study a more general scenario where a time variant frequency selective fading channel is considered, We notice that the analitical expressions for the statistical characterization of the SINR found in the previous chapter, that have enabled a simplified treatment of the system performance, no longer apply. Therefore, here we take a more practical approach and employ the BER at the receiver as performance criterion to determine whether a packet is lost or not. More specifically, a packet is considered to be successfully received if, after decoding, the number of erronenous bits is below a threshold χ. The analysis below focuses on obtaining an expression for the demodulated received signal on the desired subchannel $Y[k]$ for different retransmission strategies, the BER at the receiver is then evaluated by simulating the system from the input bit stream to the output bit stream (recall Fig. 1.3). Finally, like in the previous model, according to the HARQ protocol, retransmission of an erroneously decoded packet is performed after a time τ seconds, which in practice depends on the specific implemented retransmission protocol and on the round trip signaling times.

4.1 Signal Model

As considered in the previous section, we consider an OFDM system with N subcarriers, an input data symbols sequence $(X_0, X_1, \ldots, X_{N-1})$ corresponding to subcarriers 0,1,..., $N-1$ and bandwidth $1/T_s$, where T_s is the symbol period. For clarity of the notation, we will use in this chapter $[n]$ and $[k]$ for denoting time and frequency subscripts respectively. At the receiver, considerig a multipath fading channel consisting of L discrete paths, the received signal from M active base stations at time n can be expressed as in equation (3.2):

$$y[n] = \sum_{i=1}^{M} \sum_{l=0}^{L-1} \delta_i h_i[n, l] x_i[n - l] + w[n], \tag{4.1}$$

where: subscript i denotes different base stations, $\delta_i = (R/r_i)^{\eta/2}$ accounts for the path loss with r_i being the distance between base station i and receiver and η is the path loss exponent which depends on the specific propagation environment (Table A.1); $h_{l,i}[n]$ is a nonzero mean complex Gaussian variable

29

accounting for the channel response for the lth path; $x_{l,i}[n]$ is the nth time-sample of the trasmitted sequence from base station i for the lth path; and $w[n]$ is additive white Gaussian noise (AWGN) with power N_0.

If we further assume that the guard interval length is longer than the multipath delay of the channel $L-1$, then, once it is removed, the received signal in (4.1) can be considered as a circular convolution result of the transmitted signals and the channel. Therefore the demodulated signal on subcarrier k, $Y[k]$ after taking the FFT of the received sequence $y[n]$ reads

$$Y[k] = \sum_{i=1}^{M} \left[\delta_i \sum_{m=0}^{N-1} \sum_{l=0}^{L-1} X_i[m] H_{i,l}[k-m] e^{-j2\pi lm/N} \right] + W[k] \tag{4.2}$$

where

$$H_{i,l}[k] = \frac{1}{N} \sum_{n=0}^{N-1} h_i[n,l] e^{-j2\pi kn/N} \tag{4.3}$$

is the FFT of the time-variant multipath channel $h_i[n,l]$ and $W[k]$ denotes the FFT of noise $w[n]$. If we define:

$$a_i[k,m] = \sum_{l=0}^{L-1} H_{i,l}[k-m] e^{-j2\pi ml/N} \tag{4.4}$$

then equation (4.2) reads

$$
\begin{aligned}
Y[k] &= \sum_{i=1}^{M} \left[\delta_i \sum_{m=0}^{N-1} a_i[k,m] X_i[m] \right] + W[k] \\
&= \sum_{i=1}^{M} \left[\delta_i a_i[k,k] X_i[k] + \delta_i \sum_{m=0,m\neq k}^{N-1} X_i[m] a_i[k,m] \right] + W[k] \\
&= \sum_{i=1}^{M} \left(\delta_i \alpha_i[k] X_i[k] + \delta_i \beta_i[k] \right) + W[k],
\end{aligned}
\tag{4.5}
$$

where

$$\alpha_i[k] = a_i[k,k] \tag{4.6}$$

represents the multiplicative distortion at the desired subchannel and

$$\beta_i[k] = \sum_{m=0,m\neq k}^{N-1} X_i[m] a_i[k,m] \tag{4.7}$$

represents the ICI.

4.2 Retransmission Protocols

In this section we present the same protocols as in the previous chapter, with the exception of Protocol 1 and Protocol 3, which have already been proved to have the worst performances. Notice that, for consistency, we still refer to the remaining protocols as Protocol 2 and Protocol 4. Notice that, unlike in the previous chapter, analysis and simulation of Protocol 5 (Alamouti's STBC) can be easily performed within the framework of this new model.

4.2.1 Protocol 2

As in the previous model, this protocol combines HARQ with hard handover between adjacent base stations. Just one base station transmits at any given time and the handover is performed once the receiver approaches half the distance between base stations, so that the areas of coverage are as indicated in Fig. 3.5.

Simplifying equation (4.5) for the case of $M = 1$ active base stations, we get:

$$
\begin{aligned}
Y[k] &= \left[\delta_i a_i[k,k] X_i[k] + \delta_i \sum_{m=0, m \neq k}^{N-1} X_i[m] a_i[k,m] \right] + W[k] \\
&= \delta_i \alpha_i[k] X_i[k] + \delta_i \beta_i[k] + W[k],
\end{aligned}
\tag{4.8}
$$

where i could be either 1 or 2 depending on which base station is transmitting in the active HARQ session.

4.2.2 Protocol 4: Beamforming

In this model the beamforming is performed on the frequency domain and on each subcarrier individually. According to this, the two base stations nearest to the receiver, BS1 and BS2 transmit simultaneously the following signals for subcarrier k:

$$
\begin{aligned}
X_1[k] &= w_1[k] X[k] = \frac{a_1^*[k,k]}{|a_1[k,k]|} X[k] \\
X_2[k] &= w_2[k] X[k] = \frac{a_2^*[k,k]}{|a_2[k,k]|} X[k]
\end{aligned}
\tag{4.9}
$$

where $a_i[k,k]$ is defined in (4.4) and $w_1[k] = (a_1^*[k,k]/|a_1[k,k]|)$ and $w_2[k] = (a_2^*[k,k]/|a_2[k,k]|)$ are the weighting factors. The total power constraint is satisfied by transmitting from the two base stations at half power from respect to Protocol 2.
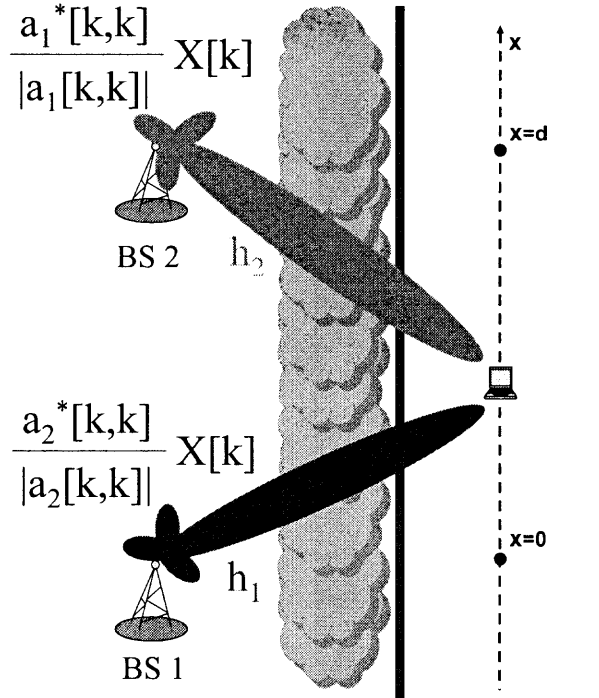
Figure 4.1 Illustration of Protocol 4 with beamforming performed on each subcarrier.

Recalling (4.5) the demodulated signal on subcarrier k for $M = 2$ active base stations reads:

$$
\begin{aligned}
Y[k] &= \sum_{i=1}^{2}\sum_{m=0}^{N-1} \delta_i a_i[k,m]w_i[m]X[m] + W[k] \qquad\qquad (4.10)\\
&= \sum_{i=1}^{2} \delta_i \left[a_i[k,k]w_i[k]X[k] + \sum_{m=0,m\neq k}^{N-1} \delta_i a_i[k,m]w_i[m]X[m] \right] + W[k]\\
&= \left(\delta_1 |a_1[k,k]| + \delta_2 |a_2[k,k]| \right) X[k]\\
&\quad + \sum_{m=0,m\neq k}^{N-1} \left[\delta_1 a_1[k,m]w_1[m] + \delta_2 a_2[k,m]w_2[m] \right] X[m] + W[k]
\end{aligned}
$$

Notice that the gain for subcarrier k has been increased compared to the gain in the previous protocol, since it is a linear combination of the gains of both channels. However notice that the ICI has been also increased.

4.2.3 Protocol 5: Alamouti's STBC

Recalling the analysis in section 3.2.5, we rewrite equations (3.26) to (3.36) for frequency selective channels. During the first symbol period, $X_1[k]$ and $X_2[k]$ are sent from BS1 and BS2 respectively for each $k = 0, 1, ..., N - 1$. During the second symbol period, $-X_2^*[k]$ and $X_1^*[k]$ are sent from BS1 and BS2 respectively for each $k = 0, 1, ..., N - 1$.
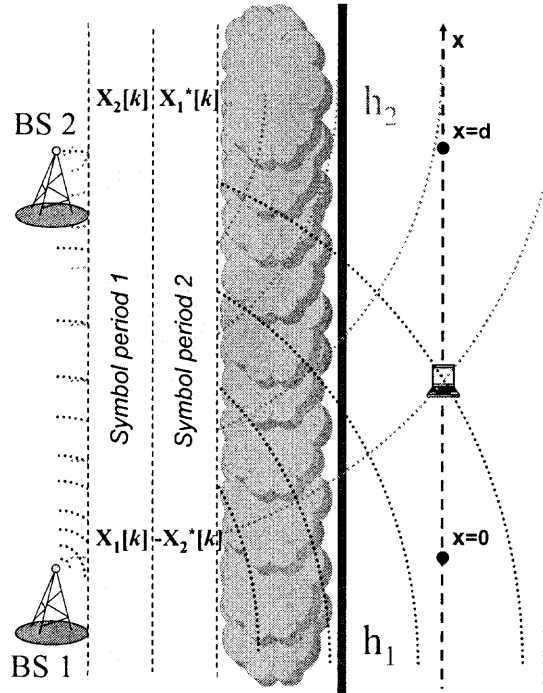
Figure 4.2 Illustration of Protocol 5 with Alamouti's technique applied in the frequency domain

At the receiver, considerig a multipath fading channel consisting of L discrete paths, the received signal from $M = 2$ active base stations at time n can be expressed as:

$$y_p[n] = \sum_{i=1}^{2} \sum_{l=0}^{L-1} \delta_{i,p} h_{i,p}[n, l] x_{i,p}[n - l] + w_p[n] \quad p = 1, 2 \tag{4.11}$$

where p denotes the pth symbol period. Notice that the received signals are a combination of the signals transmitted from both base stations. The modulated signal on subcarrier k after taking the FFT, can be expressed in the frequency domain [10] as:

$$Y_p[k] = \sum_{i=1}^{2} \sum_{m=0}^{N-1} \delta_{i,p} a_{i,p}[k, m] X_{i,p}[m] + W_p[k] \quad p = 1, 2 \tag{4.12}$$

where

$$a_{i,p}[k,m] = \sum_{l=0}^{L-1} H_{i,p,l}[k-m]e^{-j2\pi ml/N} \tag{4.13}$$

and

$$H_{i,p,l}[k] = \frac{1}{N} \sum_{n=0}^{N-1} h_{i,p}[n,l]e^{-j2\pi kn/N} \tag{4.14}$$

represents the FFT of the lth multipath component between the ith base station and the receiver during the pth symbol period.

Equation (4.12) can be expressed in matrix notation as [10]:

$$\mathbf{Y}[k] = \mathbf{A}[k,k]\mathbf{X}[k] + \sum_{m=0,m\neq k} \mathbf{A}[k,m]\mathbf{X}[m] + \mathbf{W}[k] \tag{4.15}$$

where

$$\mathbf{A}[k,m] = \begin{bmatrix} \delta_{1,1}a_{1,1}[k,m] & \delta_{2,1}a_{2,1}[k,m] \\ \delta_{2,2}a_{2,2}^*[k,m] & -\delta_{1,2}a_{1,2}^*[k,m] \end{bmatrix} ; \tag{4.16}$$

$$\mathbf{Y}[k] = \begin{bmatrix} Y_1[k] \\ Y_2^*[k] \end{bmatrix} ; \quad \mathbf{X}[k] = \begin{bmatrix} X_1[k] \\ X_2[k] \end{bmatrix} ; \quad \mathbf{W}[k] = \begin{bmatrix} W_1[k] \\ W_2^*[k] \end{bmatrix} . \tag{4.17}$$

These signals are then combined according to the Alamouti's combining scheme, this is by multiplying the received signal by $\widetilde{\mathbf{A}}^H[k]$, being $\widetilde{\mathbf{A}}[k]$ defined as:

$$\widetilde{\mathbf{A}}[k] = \begin{bmatrix} \alpha_1[k] & \alpha_2[k] \\ \alpha_2^*[k] & -\alpha_1^*[k] \end{bmatrix} \tag{4.18}$$

where

$$\alpha_1[k] = a_{1,1}[k,k] \tag{4.19}$$

$$\alpha_2[k] = a_{2,1}[k,k]. $$

Therefore if we define

$$\widetilde{\mathbf{Y}}[k] = \widetilde{\mathbf{A}}^H[k]\mathbf{Y}[k] \tag{4.20}$$

then the received signal after decoding reads

$$\widetilde{\mathbf{Y}}[k] = \rho[k]\mathbf{I}_2\mathbf{X}[k] + \mathbf{C}_{INTRA}[k]\mathbf{X}[k] + \sum_{m=0,m\neq k} \mathbf{C}_{INTER}[m]\mathbf{X}[m] + \widetilde{\mathbf{W}}[k] \qquad (4.21)$$

where

$$\rho[k] = |\alpha_1[k]|^2 + |\alpha_2[k]|^2; \qquad (4.22)$$

$\mathbf{C}_{INTRA}[k]\mathbf{X}[k]$ is the intercarrier interference (or intracodeword coupling) that shows the coupling effect between symbols in a codeword with

$$\mathbf{C}_{INTRA}[k] = \widetilde{\mathbf{A}}^H[k]\mathbf{A}_\Delta[k] \qquad (4.23)$$
$$\mathbf{A}_\Delta[k] = \mathbf{A}[k,k] - \widetilde{\mathbf{A}}[k];$$

$\sum_{m=0,m\neq k} \mathbf{C}_{INTER}[m]\mathbf{X}[m]$ is the ICI (or intercodeword coupling) that shows the coupling effect between symbols in different codewords with

$$\mathbf{C}_{INTER}[k] = \widetilde{\mathbf{A}}^H[k]\mathbf{A}[k,m] \qquad (4.24)$$

and

$$\widetilde{\mathbf{W}}[k] = \widetilde{\mathbf{A}}^H[k]\mathbf{W}[k]. \qquad (4.25)$$

Finally, the total power constraint is satisfied by transmitting from the two base stations at half power from respect to Protocol 2.

4.3 Numerical Results

As in the previous chapter, in order to compare the three protocols we consider the averaged number of retransmissions per packet over the fading distribution as the performance criterion, and evaluate it via Monte Carlo simulations. The receiver travels along the x-axis, and our simulations are focused on HARQ sessions that start within the area between BS1 and BS2. Again, we refer to the point where the HARQ session starts as x^* (recall Fig. 3.11).

While in order to simulate Protocols 2 and 4, the system depicted in Fig. 1.3 is considered, for simulation of Protocol 5 (Alamouti's STBC) the system in Fig. 3.10 is used. For all cases, an OFDM

system with N=128 subcarriers is considered and each subcarrier has been QPSK modulated. As in [10], a two-path channel with equal power and delays of 0 dB and $4Ts$ respectively is considered, with each experiencing independent Ricean fading. Clark's model was used for the Ricean fading channel simulation and it was simulated as indicated in [8 - Fig. 5.24]. The total signal power from the transmit base stations is so that $E_{total}/N_0 = 10$ dB. The carrier frequency f_c is assumed to be $f_c = 2$ GHz and the symbol period T_s is 7.8125 μs. The delay τ between the retransmissions of the same packet has been set to $\tau = 10$ ms. We have considered the path loss exponent η equal to 3. The maximum number of retransmissions L is set equal to $L = 25$. Finally, a packet is considered to be successfully received if the number of erroneous bits after decoding is lower than the 5% of the total bits transmitted ($\chi = 5\%$).

4.3.1 Performance for Fixed Initial Position $x^* = d/2$

Figures 4.3 and 4.4 show the average number of transmissions of the three protocols for two different speeds of the receiver, $v = 60$ and 210 km/h respectively, and for a specific initial position, $x^* = d/2$. As it can be seen for both speeds beamforming (protocol 4) always presents the lowest rate of transmissions followed by protocol 5 (Alamouti's STBC) and then protocol 2 (hard handover according to Fig. 3.5).
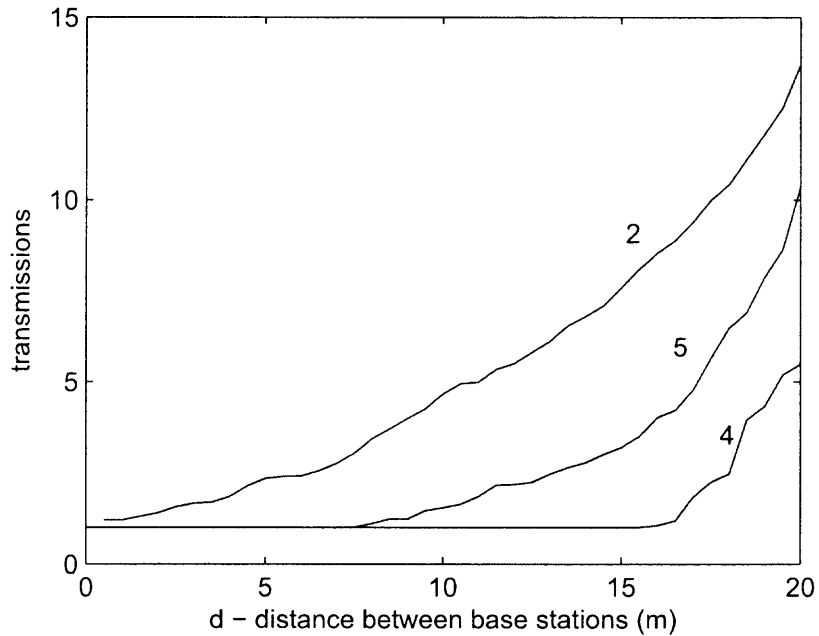

Figure 4.3 Average number of transmissions per packet for a user starting at $x^* = d/2$ and travelling with velocity v=60 km/h versus distance d between base stations.
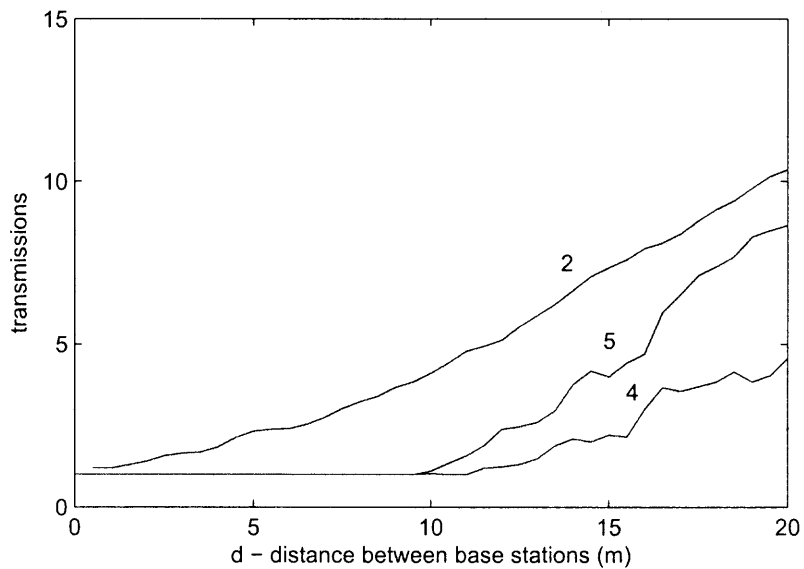
Figure 4.4 Average number of transmissions per packet for a user starting at $x^* = d/2$ and travelling with velocity v=210 km/h versus distance d between base stations.

4.3.2 Performance for Fixed $d = 20$ m

Figures 4.5 and 4.6 show the performance of the three protocols for the same two different speeds of the receiver but in this case the distance d between base stations has been fixed to $d = 20$ m and the starting point x^* varies from $x^* = 0$ to $x^* = 20$ m. As it can be seen Protocol 2 and 4 behave similarly as in the previous model for this same set of simulations. Protocol 2 has increasing number of retransmissions for starting points x^* such that handover to the second base station is not initiated within the HARQ session, and decreasing number of retransmissions after this point. On the other hand, Protocol 4 and 5 have increasing number of retransmissions for starting points x^* such that the receiver is not able to exploit the signal from the second base station within the given HARQ session due to the small received power, and decreasing number of retransmissions after this point.

4.3.3 Performance on Average Over All Initial Positions

As a final evaluation, Figures 4.7 and 4.8 show the number of retransmissions averaged over all initial positions x^* uniformly distributed between 0 and d, versus the distance d between base stations. This last set of simulations confirms the conclusions drawn before.
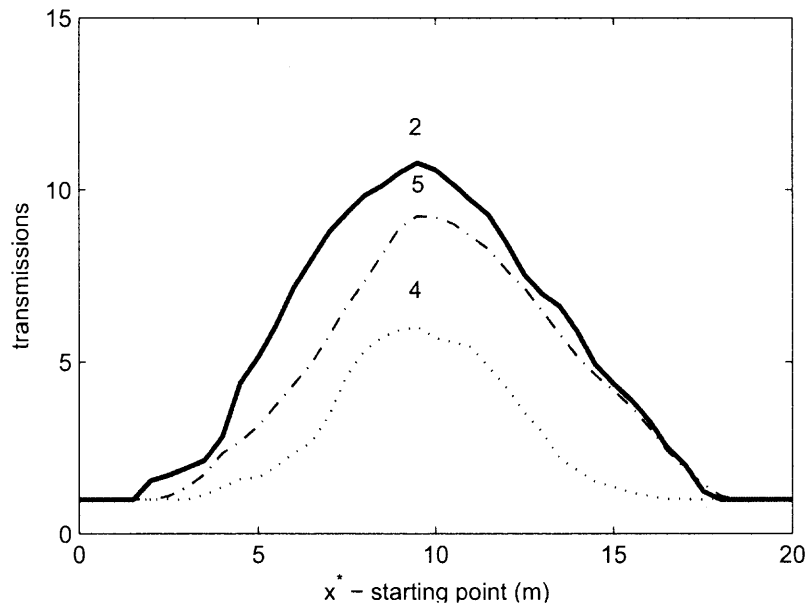
Figure 4.5 Average number of transmissions for distance between base stations $d = 20$ m and travelling with velocity v=60 km/h versus starting point x^*.

4.3.4 Remarks

Notice that, while an OFDM system with N=1024 subcarriers was considered in the first model, an OFDM system with only N=128 subcarriers has been used in this last model, since the ICI becomes inacceptably large as the number of subcarrier increases, especially in protocol 5 (Alamouti's STBC). Due this, the results obtained in the two models are not quantitative comparable between each other. However, the results obtained with the two models confirm that protocols that emploit soft handover based on beamforming outperform any other protocol in terms of number of retransmissions.
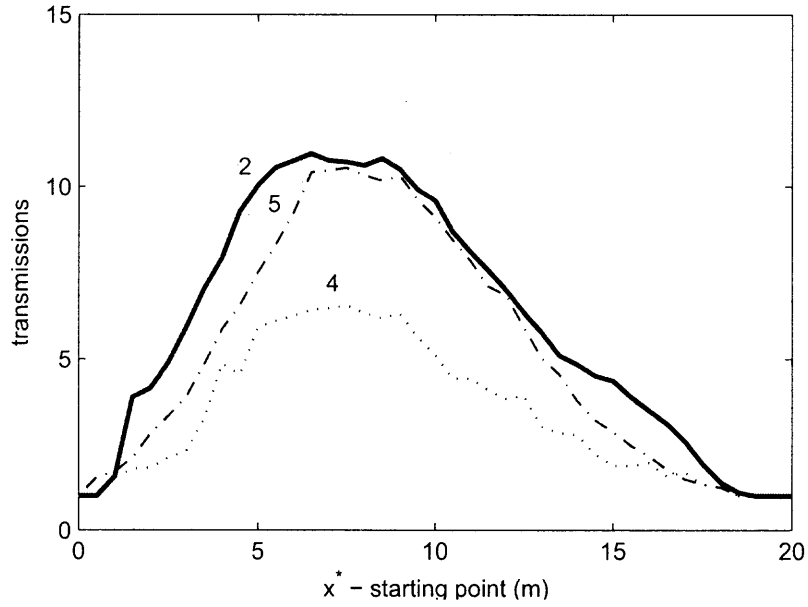
Figure 4.6 Average number of transmissions for distance between base stations $d = 20$ m and travelling with velocity v=210 km/h versus starting point x^*.

Figure 4.7 Average number of transmissions for starting point $x^* = 0$ and travelling with velocity v=60 km/h versus distance d between base stations.

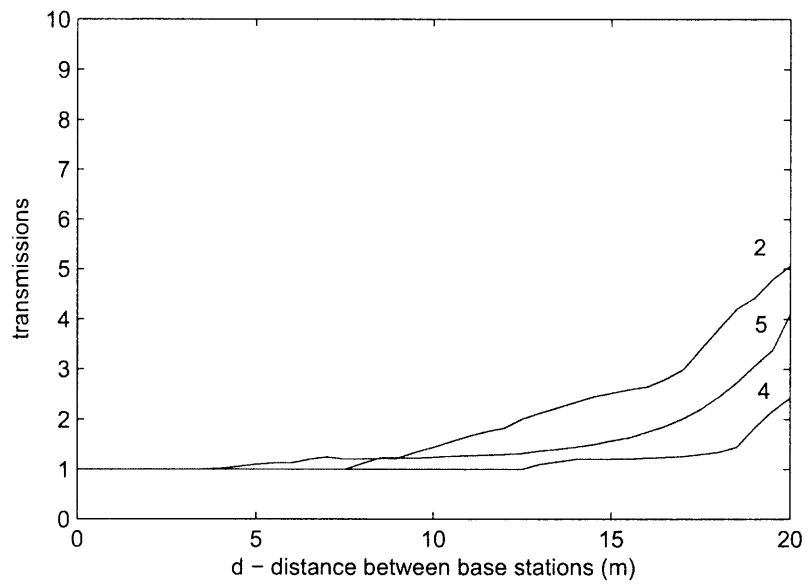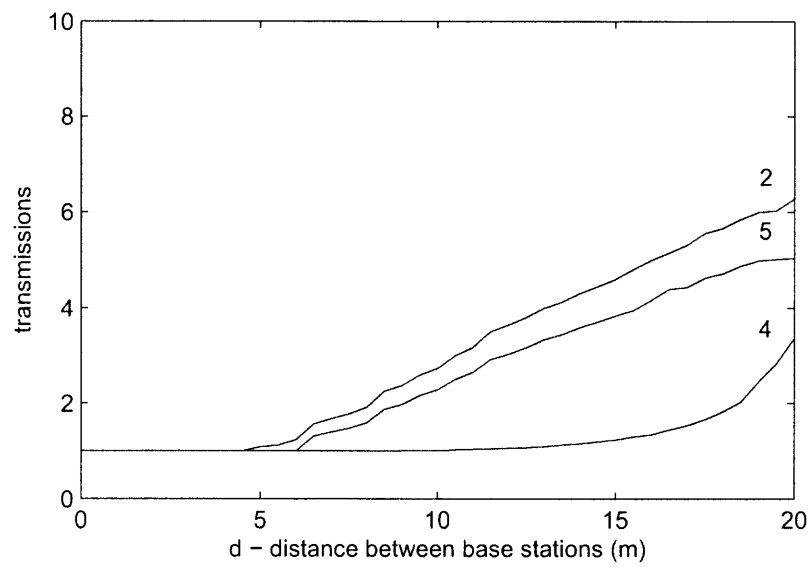**Figure 4.8** Average number of transmissions for starting point $x^* = 0$ and travelling with velocity v=210 km/h versus distance d between base stations.

CHAPTER 5

FINAL REMARKS

5.1 Conclusion

In this work, we have studied the problem of implementing HARQ protocols for communi-cations to moving receivers served by base stations placed along the path. Furthermore OFDM has been considered as modulation scheme. Typical applications of interest are vehicular or moving networks. Two different models has been presented. The first model considered a frequency nonselective channel that changes in a linear fashion during one OFDM symbol period, and it used the SINR at the receiver as performance criterion to decide when a packet is lost. The second model considered a multipath channel and used the BER at the receiver as performance criterion. Numerical results presented here have shown that, under total power constraints, hard handover strategies perform well with respect to soft handover schemes based on selection diversity protocols. Moreover, protocols that exploit space-time coding (Alamouti's STBC) outperform hard handover strategies. Finally, significant improvement can be achieved by employing soft handover based on beamforming in the presence of channel state information at the base stations.

5.2 Future Research

The work presented here has focused on the single-user case. It would be interesting to extend this work to study the multi-user case and see how the protocols presented here perform when the system has more than one receiver. Multiple access could be achieved by employing OFDMA, which is the multi-user version of the OFDM modulation scheme, and where multiple access is achieved by assigning subsets of subcarriers to individual users.

APPENDIX A

PATH LOSS EXPONENTS FOR DIFFERENT ENVIRONMENTS

Table A.1 Path loss exponents for different environments [8]

Environment	Path loss exponent, η
Free space	2
Urban area cellular radio	2.7 to 3.5
Shadowed urban cellular radio	3 to 5
In building line-of-sight	1.6 to 1.8
Obstructed in building	4 to 6
Obstructed in factories	2 to 3

APPENDIX B

PROOF OF $E[\beta_{K,1}\beta_{K,2}] = 0$ IN EQUATION (3.23)

The ICI component for subcarrier k and channel i is defined as (recall (3.9)):

$$\beta_{k,i} = \frac{1}{N} \sum_{m=0,m\neq k}^{N-1} \sum_{n=0}^{N-1} |h_{n,i}| X_{m,i} e^{-j2\pi n(k-m)/N} \tag{B.1}$$

so that:

$$
\begin{aligned}
E[\beta_{k,1}\beta_{k,2}] &= \frac{1}{N^2} E\left[\sum_{m\neq k}^{N-1}\sum_{w\neq k}^{N-1} X_{m,1} X_{w,2} \right. \\
&\qquad \left. \sum_{n=0}^{N-1}\sum_{g=0}^{N-1} |h_{n,1}||h_{g,2}| e^{\frac{j2\pi i(m-k)}{N}} e^{\frac{j2\pi g(w-k)}{N}} \right] \\
&= \frac{1}{N^2} \sum_{m\neq k}^{N-1}\sum_{w\neq k}^{N-1} E[X_{m,1} X_{w,2}] \\
&\qquad \sum_{n=0}^{N-1}\sum_{g=0}^{N-1} E[|h_{n,1}||h_{g,2}|] e^{\frac{j2\pi((m-k)n+(w-k)g)}{N}}.
\end{aligned}
\tag{B.2}
$$

Now we notice that for $m \neq w$, the expected value $E[X_{m,1}X_{w,2}]$ is 0, since $X_{m,1}$ and $X_{w,2}$ are independent zero-mean random variables, whereas for $m = w$, $E[X_{m,1}X_{w,2}] = E[X_{m,1}^2] = E_s/2$, so that equation (B.2) can be written as:

$$
\begin{aligned}
E[\beta_{k,1}\beta_{k,2}] &= \frac{E_s}{2N^2} \sum_{n=0}^{N-1}\sum_{g=0}^{N-1} E[|h_{n,1}||h_{g,2}|] \\
&\qquad \sum_{m\neq k}^{N-1} e^{\frac{j2\pi(m-k)(n+g)}{N}}.
\end{aligned}
\tag{B.3}
$$

Observing now that $|h_{n,1}|$ and $|h_{g,2}|$ are independent variables of constant mean, we can write the above expression as:

$$
\begin{aligned}
E[\beta_{k,1}\beta_{k,2}] &= \frac{E_s}{2N^2} E[|h_1||h_2|] \\
&\qquad \sum_{n=0}^{N-1}\sum_{g=0}^{N-1}\sum_{m\neq k}^{N-1} e^{\frac{j2\pi(m-k)(n+g)}{N}}
\end{aligned}
\tag{B.4}
$$

43

where the term $\sum_{n=0}^{N-1} \sum_{g=0}^{N-1} \sum_{m \neq k}^{N-1} e^{\frac{j2\pi(m-k)(n+g)}{N}}$ is the sum of equal spaced fasors over the unit circle and therefore equal to 0, thus concluding the proof.

REFERENCES

[1] A. Ghosh, D. R. Wolter, "Broadband Wireless Access with WiMax/802.16: Current Performance Benchmarks and Future Potential", *IEEE Communications Magazine*, pp 129-136, February 2005.

[2] L.Wan, V.K. Dubey, "BER Performance of OFDM System Over Frequency Nonselective Fast Ricean Fading Channels", *IEEE Communications Letters*, vol. 5, no. 1, pp 19-21, January 2001 .

[3] W.G. Jeon, K.H. Chang, Y.S. Cho, "An Equalization Technique for Orthogonal Frequency-Division Multiplexing Systems in Time-Variant Multipath Channels", *IEEE Transactions on Communications*, vol. 47, no. 1, pp 27-32, January 1999.

[4] M. Russell, G.L. Stüber, "Interchannel Interference Analysis of OFDM in a Mobile Environment", *Vehicular Technology Conference*, 1995 IEEE 45th, pp 820-824, July 1995.

[5] P. Robertson, S.Kaiser "The Effects of Doppler Spreads in OFDM(A) Mobile Radio Systems", *Vehicular Technology Conference '99-Fall*, pp. 329-333, September 1999.

[6] Y.H.Kim, I.Song, H.G. Kim, T. Chang, H.M. Kim, "Performance Analysis of a Coded OFDM System in Time-Varying Multipath Rayleigh Fading Channels", *IEEE Transactions on Vehicular Technology*, Vol. 48, no. 5, pp 1610-1615, September 1999.

[7] P. Frenger, S. Parkvall, and E. Dahlman, "Performance comparison of HARQ with chase combining and incremental redundancy for HSDPA," in *Proc. IEEE 54th Veh. Technol. Conf.*, vol. 3, Oct. 7–11, 2001, pp. 1829-1833.

[8] T.S. Rappaport, *Wireless Communications: Principles and Practice*, Englewood Cliffs New York, Prentice-Hall, 1996.

[9] S. M. Alamouti, "A Simple Transmit Diversity Technique for Wireless Communications", *IEEE Journal on Selected Areas in Communications*, vol. 16, no. 8, pp. 1451-1458, October 1998.

[10] J. Kim, R.W. Health, and E.J. Powers, "Receiver Designs for Alamouti Coded OFDM Systems in Fast Fading Channels", *IEEE Transactions on Wireless Communications*, vol. 14, no. 2, pp. 550-559, March 2005.